CHAPTER 8

Regional and Landscape Ecological Analysis

I. INTRODUCTION

In Chapter 7 we introduced principles and special techniques that allow the extension of ecosystem analyses to the scale of landscapes and regions. We concentrated on techniques to quantify the abiotic variables of the landscape and meteorological variables that drive the ecosystem. Techniques for quantifying directly observable or inferable state variables of the ecosystem were also identified. In this chapter we assemble these spatial scaling techniques to address landscape-level processes. We also integrate various ecological simulation models into our spatial analysis to provide capability for temporal extrapolation. This chapter presents a variety of landscape ecological studies that vary in the questions being asked and the degree of interconnections required for solution. Returning to the principles illustrated in Fig. 7.1, we evaluate the relative importance of spatial coupling in the vertical and horizontal directions, and the temporal dynamics appropriate to an array of regional scale analyses. Regardless of what spatial connections or time scales are

chosen, we must incorporate process-level understanding to extend quantitative predictions to landscape scales.

Of equal importance, the studies demonstrate a capacity for real-time monitoring or future projection of ecosystem processes. Some resource management decisions require real-time information, such as those involving fire management, grazing intensity, or flood control. Other resource management decisions depend on the implications of projecting ecosystem responses decades into the future. How will streamflow and wildlife habitat change if a proposed harvest plan or prescribed fire is implemented in a watershed? Land managers currently make many decisions based on past experiences or local field trials, because those are the only options available when a decision is required. The capacity to demonstrate the potential implications of various policy decisions is perhaps the most valuable contribution ecosystem analysis can provide to decision makers. Making such contributions, however, requires geographically explicit analyses over a range of time frames. Ecological understanding that is not presented in these terms can provide little direct help in land management. We feel that geographically referenced predictive responses, resting on a foundation of process models, provide a consistent and useful summary of ecological information that can be made available to a wide range of managers. Although models will continue to be improved as knowledge increases, the most immediate challenge is to present predictions in a more graphic, understandable form. To meet this challenge, it is essential that model developers work closely with the land managers who must ultimately interpret and be responsible for implementing policies.

The first section of this chapter covers ecological processes where the horizontal connections are strong and the vertical links are weak. Because of the longer time constant associated with many horizontal connections, temporal dynamics are often not emphasized. Detection of land cover changes and wildlife habitat analysis are examples of problems with these connective properties. In the next section, the emphasis shifts to subjects where the vertical and temporal processes are strongly coupled, such as interactions between vegetation and the atmosphere. The final section covers problems where both horizontal and vertical connections are required, and where systems are also temporally dynamic. These analyses quantify both the change in *structure* through time as stands develop, are disturbed, or are eliminated, and changes in rates of *functions,* represented by the movement of water, carbon, and nutrients across the landscape (regional biogeochemistry). These models present land managers a tool to depict future changes in the landscape based on various policy options before implementing them.

II. HORIZONTAL CONNECTIONS: BIOTIC ANALYSIS OF FOREST PATTERNS

In Chapter 6 we discussed how certain types and frequencies of disturbance were a natural and continuous part of the development of forest ecosystems. Forest disturbances at the local level can result from the activities of resident animals, insects, and pathogens. At the landscape scale, forest disturbances are more commonly a human activity, through harvesting, establishment of large exotic plantations, converting forests to farms, air pollution, and urbanization. Some natural disturbances such as insect defoliation, wildfires,

floods, and windstorms also can impact large areas. The spatial extent and frequency of various types of disturbances are important to quantify. It is instructive to compare the natural rates and magnitudes of disturbance with more recent human activities because both the timing and spatial extent of human disturbances can frequently be controlled. It may prove desirable to match management-related disturbances to those for which natural systems are well adapted.

It is becoming increasingly difficult to decipher original forest patterns because so little land remains in a relatively pristine state. Parks and wilderness areas can provide some means to compare contrasting management policies on adjacent landscapes. However, if these park areas have had wildfire protection or controlled populations of native animals, then the resulting forest cover is rather atypical because of the interruption of natural disturbances. A satellite image provides vivid documentation of disturbance associated with logging activities on National Forest land that is in contrast with adjacent parkland of Yellowstone National Park (Fig. 8.1). Extensive clear-cut patches are visible in the national forest, but the *natural* parkland was also extensively altered in 1988 when a wildfire burned 321,000 ha of predominantly old pine forest. The large extent of the 1988 fires was caused by a century of fire suppression causing a buildup of spatially continuous fuels that would never have occurred with the annual mosaic of small fires typical of that region. Thus, differing management strategies have produced dramatically different landscapes, but neither has retained the age classes and structural distributions of trees typical of an earlier, more natural landscape.

The significance of a disturbance can only be measured in the context of the landscape of interest and the ecological resilience of the local forests. M. G. Turner *et al.* (1993) designed a general analysis to evaluate the significance of disturbances at any spatial scale, called a state–space diagram (Fig. 8.2). Within this general framework, any time/space combination of landscape disturbance can be evaluated, from a year to a century and from a few hectares to thousands of square kilometers. The critical spatial measure of significance is the fraction of the defined landscape that is influenced by the disturbance (x axis). Different disturbances have varying levels of severity or temporal consequences to the original forest (e.g., the influence of a wildfire lasts much longer than a single defoliation). Thus, Turner *et al.* quantify temporal disturbance as a ratio of the disturbance interval to the time it will take that forest to return to its prior state (y axis). Defoliation of a few hectares of trees in a thousand square kilometer landscape would be quantified with both x and y values approaching zero, which represents a disturbance of limited significance in both time and space. The wildfire in Yellowstone Park in 1988 that burned 36% of the area has a statistical return interval of 300 years, so will leave its imprint on that landscape for centuries.

A. Temporal Changes in Forest Cover

The magnitude of human-induced landscape disturbance is often difficult to determine, and few studies have been able to quantify long-term changes in forest cover. White and Mladenoff (1994) compared the forest cover of a 9600-ha area of northern Wisconsin from pre-European settlement (1860s) to postsettlement (1930s) and the present (1989). Presettlement forest cover was estimated from U.S. Government survey records,

FIGURE 8.1. A Landsat TM image acquired in July 1991, clearly reveals the boundary between Yellowstone National Park and adjacent National Forest lands in the northern Rocky Mountains. Timber harvesting has been extensive on the National Forest lands while this activity was prohibited in the national park land. Wildfires were actively suppressed in both areas for nearly a century, resulting in almost no regular landscape-scale forest disturbance in Yellowstone National Park until the summer of 1988 when a 321,000-ha wildfire burned across much of the fuel-rich landscape within the park boundary.

postsettlement forest cover was derived from a county inventory map in 1931, and 1989 forest cover was interpreted from aerial photography. The area occupied by old-growth forest was reduced progressively from 100 to 23 to 6% from 1860 to 1989 (Table 8.1). Early pioneer species covered 50% of the area in 1931, and by 1989 over 90% of the landscape supported mixed hardwood and conifer second-growth forests.

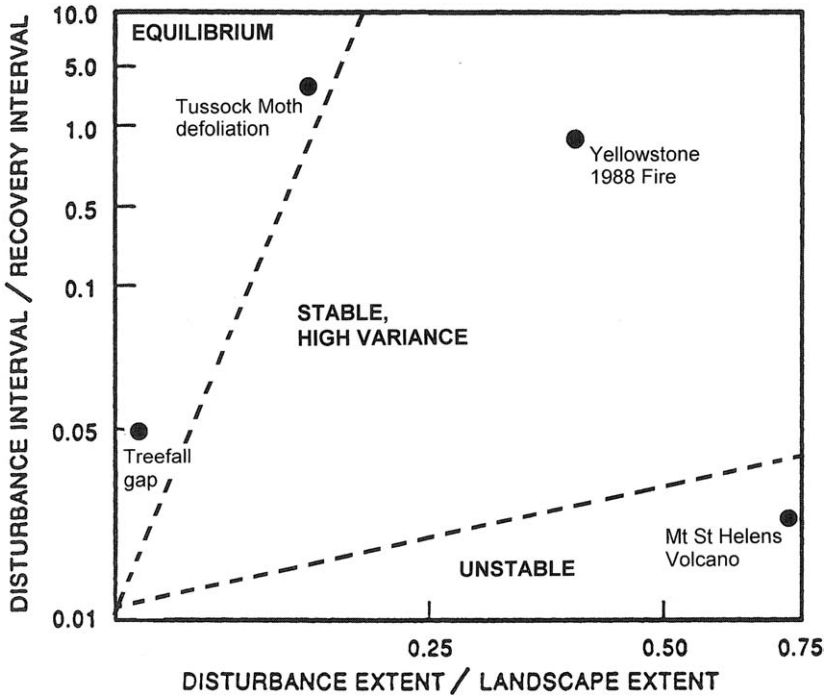

FIGURE 8.2. State–space diagram that evaluates landscape disturbance and dynamics across any spatial and temporal scales. The spatial parameter *S*, on the *x* axis, defines a disturbance as a fraction of the landscape of interest, regardless of size. The temporal parameter *T* is the ratio between the disturbance interval and the time required for the forest to recover to a mature state. When a disturbance interval is long relative to the recovery time and a small fraction of the landscape is involved, the system may be considered stable or at equilibrium. A disturbance interval comparable to the recovery interval, and affecting a large portion of the landscape, can be considered stable but with high variance. Disturbance intervals much shorter than the recovery interval and that influence a large proportion of the landscape may lead to an unstable system that shifts to another state. (From M. G. Turner *et al.*, 1993.)

TABLE 8.1
Compositional Change in Forest Type on a 9600-ha Landscape in Wisconsin over 130 years[a]

Forest type	1860	1931	1989
Pin cherry	—	37.2%	2.3%
Mixed hardwood	—	13.7%	21.8%
Mixed conifer	—	0.5%	10.3%
Hardwood/conifer	—	5.9%	29.4%
Northern hardwood	—	19.4%	30.5%
Old growth hemlock/hardwood	22.5%	—	—
Old growth hemlock	46.2%	7.2%	3.7%
Old growth hardwood	31.4%	16.1%	1.9%

[a]From White and Mladenoff (1994).

Landsat satellite data are now available from 1972 to the present for most areas of the world, so images from multiple dates can detect changes in forest cover during this recent era. Hall *et al.* (1991) compared forest cover change rates over a 10-year period in a managed forest and wilderness areas of a 900-km^2 region of Minnesota. They found that regenerating clear-cuts in the managed forest increased from 15 to 22% of the land area during the 10-year period. Eleven to thirteen percent of the wilderness area was in early stages of forest development, a result of fire and natural tree mortality. Hall *et al.* estimated that the managed forest had an interval between establishment and harvesting one-fifth the length of the interval associated with natural fires in a wilderness area. The frequency of natural fires, however, has also been significantly diminished through fire suppression activities. Frelich and Reich (1995) found that the fire frequency of a 234-km^2 region of cold temperate forest of Minnesota has changed from 1 in 50–100 years to 1 in >1000 years because of fire suppression. In some forests, the natural fire frequency can be mimicked by harvest rates and aid in managing for reasonably natural forest dynamics. Gruell (1983) provided photographic evidence of the invasion of forests over the twentieth century into grasslands in many arid areas of the northern Rocky Mountains of the United States. Fire suppression and control of grazing are the primary management actions that have resulted in this land cover change (see Fig. 6.4).

Cohen *et al.* (1995) estimated that 15.3% of the 10.4 million ha of forested land of the Pacific Northwest was harvested between 1972 and 1991, an average harvest rate of 0.8% of the area per year. In contrast, the much-publicized clearing rates in the Amazon have been documented at only 0.4% of the area per year (Skole and Tucker, 1993). Both of these studies illustrate that satellite data can provide a more repeatable and unbiased estimate than ground surveys of deforestation. Of course, the more critical analysis for forest management is the fraction of landscape *permanently* deforested and converted to urban or agriculture use. Rates of forest regrowth are not so clearly quantified by satellite imagery because the change in land cover is gradual as regenerating trees reoccupy an area.

A challenge for retaining a semblance of natural landscape dynamics may be to manage the spatial size, distribution, and timing of harvesting activities to more resemble natural disturbance processes. By tracking the trajectory of landscape change throughout recent history we attempt to project the rate of future change. Extrapolating these recorded rates of landscape change into the future rests on an implicit assumption that external conditions (population pressure, lumber prices, climate, etc.) will remain similar to those in the past. When this assumption is unwarranted, more complicated analyses are required to make future projections. Thus, past trends and rates of change in landscape patterns are a necessary precursor to evaluating future trends, but insufficient given the likelihood of additional changes in external conditions.

B. Quantifying Spatial Heterogeneity

The landscape displays structural heterogeneity beyond that recognized within groups of stands. Forest cutting is the means by which land managers most commonly affect the structural heterogeneity of landscapes, either purposefully or inadvertently. Franklin and Forman (1987) illustrated the relationship between different idealized stand cutting patterns and the resulting patch sizes and edge lengths, both critical factors in defining wildlife

habitat. Their analysis showed that as cutting unit size is decreased, the patch size of undisturbed area also decreases because more land must be entered to sustain a fixed yield of forest products. Additionally, cutting unit border length increases. One cannot state that any specific cutting pattern is "best" because preserving large patches for spotted owl habitat would reduce edge habitat along cutting boundaries favorable for producing forage and cover for deer.

Spies *et al.* (1994) found that the percentage of old-growth closed canopy forest decreased from 71 to 58% between 1972 and 1988 on a 2600-km^2 forested area studied in the center of the Oregon transect area (Fig. 8.3). Spies *et al.* also found that the size of contiguous uncut patches optimal for certain wildlife habitat declined from 160 to 62 ha, and edge density increased from 1.9 to 2.5 km^{-2} during the 16-year period. The disturbance rate for this region was 1.2%/year, or a recurrence time of 84 years. This suggests that although the current harvest rate is reasonably near the natural disturbance frequency, current forest management is increasing fragmentation and reducing the size of uncut patches.

Li *et al.* (1993) developed a simulation model that also allows constraints from streams and roads to be included in the spatial analysis of landscape heterogeneity. In simulating the habitat fragmentation produced by different forest cutting patterns, Li *et al.* (1993) found that the widely used method of placing many small clear-cuts in staggered setting produced the maximum landscape fragmentation. Wallin *et al.* (1994) used a simulation of different stand cutting patterns and timings to illustrate the interaction between clear-cut size and cutting frequency in determining the long-term landscape pattern of age-class heterogeneity in western Oregon transect forests. Gustafson and Crow (1994) evaluated the influence of different sizes and distributions of clear-cuts on bird habitat in Indiana. Their conclusions illustrate that in order to sustain a given harvest level and simultaneously retain bird habitat, clear-cuts must be aggregated to larger units. However, their recommendations may not apply to ungulate species, such as deer and elk, which tend to prefer edge habitat, foraging in recently cleared areas on successional forbs, but hiding and resting in adjacent closed canopy forests.

C. Disturbance Propagation

The propagation of disturbances is rarely random across a forested landscape. Harvested areas are usually adjacent to a road network. Disturbance by fire or wind is driven by topography and microclimate conditions, and insect epidemics spread rapidly to adjacent stands with low growth efficiencies. Models representing the explicit spatial propagation and timing of these disturbances are now being built, although few complete studies are available in the literature (Roberts, 1996a,b). The spread of balsam wooly aphid in the Appalachian Mountains was evaluated by considering population dynamics of both the aphid and the host tree, Fraser fir, and the biophysical conditions that encourage spread (Dale *et al.*, 1991). Johnston and Naiman (1990) evaluated the history of beaver pond alteration on the hydrology and vegetation at Voyageurs National Park, Minnesota. They found that from 1940 to 1986 analysis of aerial photography of a 250-km^2 area showed beaver ponds increased from 1 to 13% of the landscape, and the beaver population in 1986 was 1 colony km^{-2}. This analysis can be used directly for making management

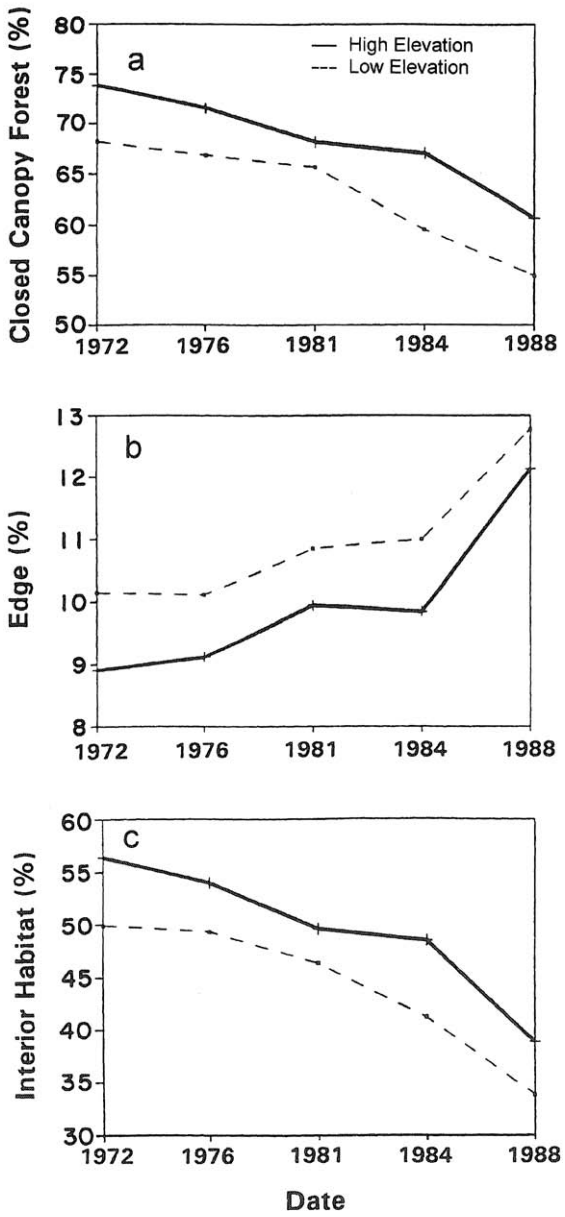

FIGURE 8.3. Reduction in closed canopy conifer forest and interior forest habitat, and resulting increase in percentage of edge, for a 2600-km^2 landscape in Oregon for the period 1972–1988 (Spies *et al.*, 1994). Landsat imagery served as the basis to classify the landscape into conifer forest versus nonforest status at 4- to 5-year intervals, with an accuracy of 91%. High elevation areas (>914 m) are primarily public land, which include 7% in wilderness areas where forest cutting is prohibited. Low elevation land (<914 m) has a mixture of public and private ownership. Over the 16-year study, conversion of areas supporting mature forests (predominantly by clear-cutting or wildfires) averaged 0.2, 1.2, and 3.9% per year for wilderness, public, and private forestland, respectively. These observed harvest rates equal or exceed reported rates in the Amazon basin (Skole and Tucker, 1993). The rates of *regrowth* are of equal importance in determining the net change in forest cover and NPP, but they are often not reported. The increase in edge resulting from harvesting activity represents a habitat improvement for deer but a detriment for spotted owls, illustrating the differential habitat requirements of wildlife and the conflicts inherent in land management. (From Spies *et al.*, 1994.)

decisions of whether the measured beaver density can be sustained or should be reduced.

D. Wildlife Habitat Analysis and Spatially Explicit Population Modeling

Evaluating wildlife habitat requires consideration of physical features of the landscape including microclimate, structural and community relationships of the vegetation, and the physiology and behavior patterns of the target organism. Habitat criteria have different levels of priority; some factors are essential while others are preferred but not required, and each animal needs different habitat, which further complicates landscape analysis. Possibly the most difficult challenge in landscape analysis involves following the movement of organisms within a complex landscape. Such analyses require "spatially explicit population models" (Dunning *et al.*, 1995). Population models have typically simplified the analysis by concentrating on the horizontal biotic interactions across ecosystem boundaries shown in Fig. 7.1, and by evaluating the vertical atmospheric and hydroedaphic processes in very simple ways or not at all. Emphasis is on the habitat quality for the organism, for example, evaluating winter thermal vegetation cover rather than absolute temperatures. Population-based models define a population for each landscape cell, so are more appropriate for abundant organisms like insects or birds, and simulate their collective movement in the landscape through time (Dunning *et al.*, 1995).

An analysis of bald eagle nesting habitat in a Montana basin began with a requirement of proximity to rivers or lakes where the primary food supplies are found (see Plate 4). A secondary priority was relatively flat terrain at low elevation in the basin, as these are not high mountain birds. The third criterion was mature forests with nearly complete canopy closure in blocks of at least 8 ha. With sequential queries of georeferenced databases of hydrography, topography, and vegetation, the intersection of criteria produced a map of probable bald eagle nesting habitat, identifying key areas of the landscape that may require special management.

A classic resource management conflict has developed around the northern spotted owl in the forests of the Pacific Northwest, including the Oregon transect area (Fig. 1.4). Prime habitat for the spotted owl is old-growth forests, yet harvest rates from 0.9 to 5.4% of the area per year since World War II had measurably reduced the old-growth forests to the point that the owl was legally defined as a "threatened species" in 1990 (Noon and McKelvey, 1996). Lamberson *et al.* (1992) proposed an array of habitat conservation areas to enhance owl populations. Extensive landscape simulations were completed to evaluate the size, shape, and proximity of these habitat blocks that would be necessary to sustain the owl population at various levels (Noon and McKelvey, 1996). Following these analyses, decisions that reduced harvest rates on millions of hectares of forested land were made that had an international impact on wood commodity values.

Hansen *et al.* (1993) combined the landscape fragmentation model of Li *et al.* (1993) with a forest gap model (Fig. 5.17) to explore the consequences of different land management objectives on future bird habitat trends. Four management alternatives were tested on a 3300-ha watershed in western Oregon, including a natural fire regime (no fire suppression), an intensive wood production alternative with 70-year harvest frequency, a multiple-use alternative with 140-year harvest frequency and larger cutting blocks, and

finally a no action alternative of letting the current landscape develop without harvesting. Simulations of forest stand development from the present for 140 years into the future were evaluated for stand conditions that provide suitable bird habitat for each alternative. All alternatives except the intensive wood production scenario retained suitable bird habitat after 140 years (Fig. 8.4). It would he difficult to perform this evaluation with so many landscape, forest, and wildlife factors and multiple management objectives without computer models.

Individual-based models track the location on the landscape of each individual at each time step. M. G. Turner *et al.* (1993, 1994) and Pearson *et al.* (1995) report on extended studies of large ungulate populations (elk, moose, deer, and bison) in Yellowstone National Park. Their analyses first quantified the landscape topography, habitat types, fire history, and forage distribution. Then initial population data for the ungulates including age, size, sex, and spatial distribution were defined. A snowpack simulation was then run to allow computation of animal foraging behavior based on snow depth and forage availability through the winter. Model emphasis is on animal energetics for survival, not hydrologic dynamics of the snowpack. Interactions among weather conditions as quantified by snow depth, fire size and spatial distribution, and foraging success of animals were evaluated with simulation experiments that would require decades of field studies to develop similar insights. Simulations showed that fires burning single large blocks, followed by a severe winter, could induce high mortality rates for an elk herd, because of the lack of forage and the difficulty animals would experience in moving through deep snowpack to search for food. The simulations indicated that future prescribed burning in this ecosystem should be distributed as small patches if the primary goal is to maintain a large elk herd. That objective would increase landscape fragmentation but would achieve park management goals of minimizing fire danger and maximizing ungulate populations (Turner *et al.*, 1995).

It is worth again noting that fragmentation of a forested landscape recommended for sustaining large populations of ungulates would be in conflict with management objectives that seek to favor large populations of some species of birds which require unbroken blocks of forests. Most land managers must balance concerns about wildlife with timber production, grazing, and watershed considerations. For these reasons the ability to evaluate the likely impact of various policies through landscape simulations before implementation has special merit. Although the landscape models available are still far from ideal, each assumption and calculation is explicit and so can be challenged and modified. When managers are considering multiple options that will shape the landscape a century into the future, decisions made must be based on the best evaluation possible.

Stable isotopes can offer a different and unique perspective for the analysis of animal habitats. The preferred home ranges and their seasonal or interannual variation can be confirmed through analyses of the isotopic composition of animal tissues such as bone, teeth, horn, and other organs. For example, Ambrose and DeNiro (1986) deduced the long-term habitat distributions of 43 species of East African mammals from the stable carbon and nitrogen isotope ratios extracted from bone collagen. Differences in the Sr, Pb, and N isotopic composition of soils were also reflected in diets of elephants, whose tusks provided a unique multiple-isotopic signature related to the distribution of herds

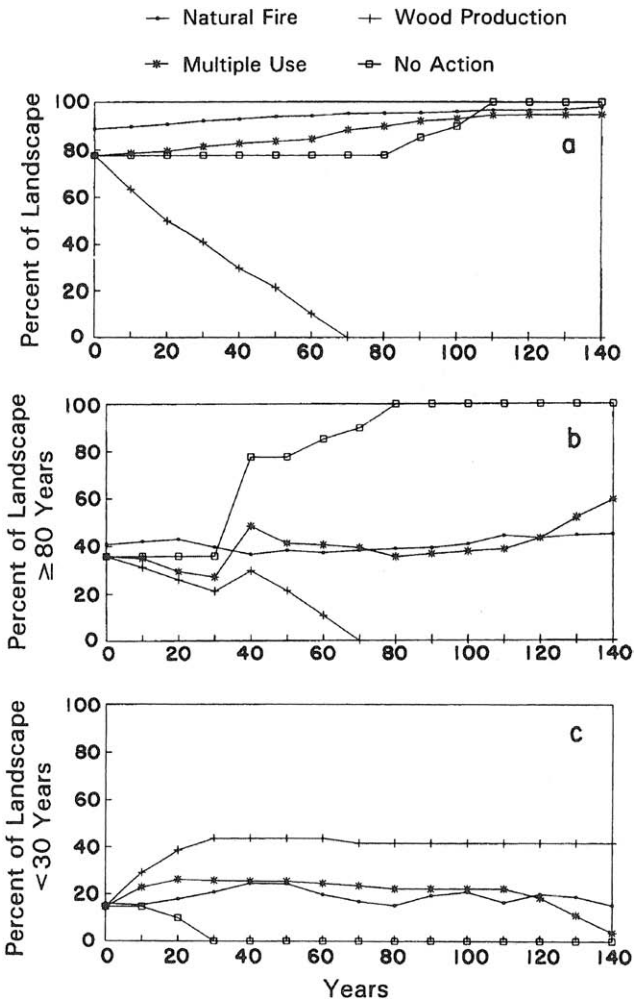

FIGURE 8.4. Simulation of change in forest structure and resulting bird habitat suitability for a 3300-ha watershed in western Oregon under four management scenarios, beginning with the current landscape and extending for 140 years into the future. Variations in fire frequency and the size and frequency of forest harvests were simulated as alternative management policies. The resulting percent distribution of the landscape under different management scenarios is shown in (a). The percentage of the landscape in key age classes representing mature individuals (≥80 years) is shown in (b) and seral stands <30 years old in (c) through the 140-year simulation. The importance of these stand ages and spatial distributions varies with bird species. (From Hansen *et al.*, 1993.)

across much of Africa (Van der Merwe *et al.*, 1990; Vogel *et al.*, 1990). Smaller animals, of course, have less extensive distributions but still often differ in their isotopic composition based on dietary selections related to marine and terrestrial food sources (Grupe and Krueger, 1990; Angerbjörn *et al.*, 1994).

III. VERTICAL CONNECTIONS: FOREST–ATMOSPHERE INTERACTIONS

The first scale of forest–atmosphere interactions are the one-dimensional or stand-level Soil–Vegetation–Atmosphere–Transfer (SVAT) models discussed in Chapters 2 and 3. In Chapter 7 we explained the representation of meteorological conditions across a landscape, using models such as MT-CLIM to extrapolate measured microclimate conditions across complex terrain. However, MT-CLIM and similar climatological models do not analyze the dynamic interaction between the forested landscape and the atmosphere. How forests respond to atmospheric dynamics is well understood at local scales from micrometeorological studies (Chapter 2). We also appreciate that advected energy and momentum are distributed across the landscape in direct response to local topography and surface conditions. Forest responses at regional scales, however, are less well known, and the influences that forests exert back on the atmosphere are particularly poorly understood.

A. Regional Forest–Atmosphere Interactions

New modeling analyses that integrate a regional scale biospheric gas and energy exchange model with a mesoscale dynamic meteorology model are providing evidence that extensive forest cutting produces a highly fractured canopy energy exchange surface; this intensifies atmospheric turbulence and thunderstorm activity over scales of tens to hundreds of kilometers (Pielke *et al.*, 1997). Pielke *et al.* suggest that thunderstorm activity in Georgia may have increased from presettlement times as a result of land conversion from continuous forests to interspersed 10- to 40-ha blocks of forest, fields, and urban areas. Forests consume the majority of incoming solar energy in evapotranspiration while agriculture and urban landscapes generate more sensible heat, which initiates the vertical convection columns that spawn thunderstorms (Fig. 8.5). This appreciation of the role of forest cutting patterns on local severe weather and the reduction of sensible heat transfer into the atmosphere may help justify not only more wide scale reforestation efforts but also tree planting and the establishment of more parks in large cites.

B. Regional Drought Analysis

Satellites allow a landscape view of the forest, but the reflected and emitted signals produced from the landscape and transformed into digital imagery often fall short of quantifying vegetation responses of interest. Vegetation development in the spring and leaf senescence in the autumn can be well represented by simple vegetation indices such as NDVI. However, the onset of seasonal drought may not be directly observable, particularly in evergreen forests. Drought influences canopy gas exchange, productivity, fire danger, grazing capacity, and wildlife survival in many forests of the world. If frequent, geographi-

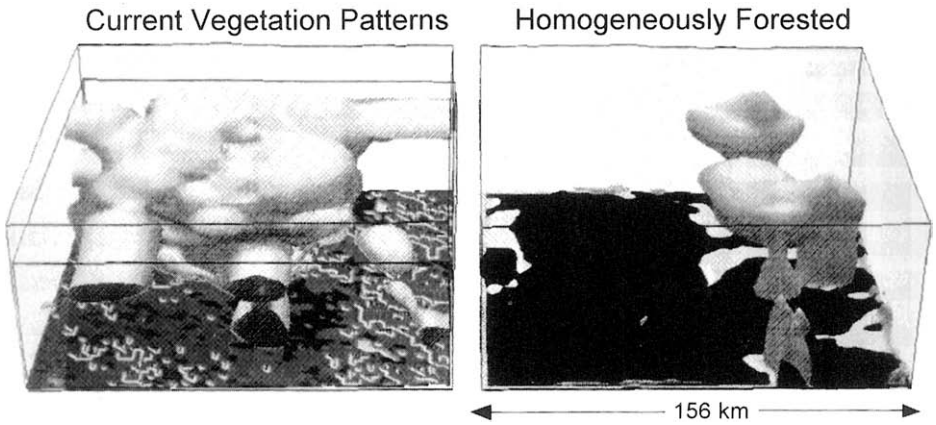

FIGURE 8.5. Simulation of afternoon convective thunderstorm development for 26 July 1987 at 1400 hr local time in central Georgia simulated with RAMS (Regional Atmospheric Modeling System). The simulation contrasts diurnal mesoscale meteorology of the current fragmented forest/farm/urban landscape mosaic with a homogeneous forest similar to a pre-colonial settlement condition (Pielke *et al.*, 1997). This analysis suggests that mesoscale turbulence and thunderstorm development have been accelerated by increasing the heterogeneity of forest land cover over the last few centuries. (From Pielke *et al.*, 1997.)

cally explicit data were available on the severity of drought, some advanced planning to minimize the impact of climatic variation would be possible.

The principles introduced in Chapter 7 to define a surface resistance from the ratio T_s/NDVI from the AVHRR satellite can be applied to display regional scale drought conditions throughout the growing season. Nemani *et al.* (1993a) developed algorithms for screening out clouds, snow, open water, and other confounding effects from the raw T_s/NDVI relationship shown in Fig. 7.11, and then computed the slope relationship to quantify surface resistance in Fig. 7.13. This automated procedure was then extended to calculate seasonal surface resistance for the continental United States for the extremely dry summer of 1988 and to contrast these values with the more normal summer of 1989 (see Plate 5). The seasonal surface resistance was converted to water deficit units and compared with the Crop Moisture Index, computed from surface meteorological data by the National Weather Service, for the summer of 1990. A high correlation was found between the standard Crop Moisture Index and the satellite-derived drought index ($r^2 = 0.83$), but the satellite-derived index can be computed more quickly and with greater spatial accuracy (Nemani *et al.*, 1993a). This satellite-derived drought index has been produced routinely by the NASA Earth Observing System program since 2000.

C. Fire Dynamics

Wildfire suppression costs at least $700 million per year in the United States alone, so any improvement in fire forecasting and management would have immediate utility and financial benefits. Fire danger, the risk of an uncontrolled ignition, has historically been computed in the United States from surface weather and fuel moisture conditions using the

National Fire Danger Rating System (Burgan, 1988). This system provides computations of fire danger from the stations of measurement and does simple extrapolation to provide continuous maps across the landscape. The satellite-derived surface resistance calculated by Nemani and Running (1989b) and Nemani *et al.* (1993a) can be translated into a fire danger index that provides an automated and spatially continuous mapping of the danger of fire ignition, integrating both the surface meteorology and the vegetation energy partitioning condition related to stress and fuel flammability. Vidal *et al.* (1994) applied a derivation of the algorithm used for Plate 5 to evaluate fire ignitions during the summers of 1990 and 1991 (when 537,000 ha burned in the Mediterranean region). The satellite-derived fire risk corresponded with the dates of observed fire ignitions in two study areas of southern France.

Fire ignition and behavior are controlled by available fuel, current meteorological conditions, and topography and have been well quantified (Rothermel, 1972). Subsequent fire spread is inherently a spatially defined problem that must integrate the georeferenced location of fuels and spatial pattern of the forest on the landscape, with the dynamic meteorology that defines the combustibility of the fuels and moves the fire across the landscape (Keane *et al.*, 1996a,b). Daily AVHRR satellite data have been used to follow fire spread, but the 1 km spatial resolution, severe changes in viewing angle from day-to-day images, and interference by smoke makes this technique useful for large fires only (Chuvieco and Martin, 1994).

Accurate mapping of the extent of large fires is also valuable for determining timber volume losses, reforestation requirements, wildlife habitat changes, hydrologic risks, and atmospheric emissions. The black, charred surface of a completely burned forest can be easily differentiated from green vegetation in visible wavelengths. However, forests with interspersed burned and unburned patches cannot be evaluated so easily. Kasischke and French (1995) were able to detect 78% of the 1.9 million ha burned by fires in Alaska during 1990 and 1991, many in remote and uninhabited areas where ground surveillance was impossible. Turner and Romme (1994) evaluated the role of preexisting stand structure patterns in crown fire spread, and the resulting mosaic produced by fires in Yellowstone National Park. The spatial distribution of burned areas influences winter elk survival, as discussed in the previous section. While acknowledging the tremendous destructive potential of wildfires, we now recognize many beneficial effects of fire on ecosystems that justify prescribing controlled fires or sometimes allowing wildfires to burn to perpetuate the more natural pattern in historically fire-dominated landscapes.

IV. VERTICAL AND HORIZONTAL CONNECTIONS: REGIONAL BIOGEOCHEMISTRY

Analysis of forest biogeochemistry at the regional scale involves vertical connections to the atmosphere as driving variables and drainage dynamics into the soil, horizontal connections between adjacent stands that influence hydrologic partitioning, and finally time dimensions from subdaily intense storms to decadal shifts in hydrology and geochemistry as stands develop. This section explores a range of regional biogeochemistry studies focused on hydrologic processes.

A. Watershed Hydrologic Balance

The most important activity of watershed scale hydrology is accurate calculation of stream and river discharges. Knowledge of river flow dynamics is required for flood forecasting, irrigation scheduling, hydroelectric power operation, and water quality issues such as temperature, oxygenation, and dilution of pollutants. The headwaters of most major river systems are in forested landscapes, and thus the management of those areas influences the quantity, quality, and timing of river flows. Near-term forecasting of streamflow relies on accurate and geographically explicit monitoring of current snowpack and precipitation, information now often transmitted from field sites to office computers instantaneously by satellite. Projections of streamflow require representation of surface heterogeneity of topography, soils, and vegetation in a realistic way. In Chapter 7 we introduced the components of a Regional Hydroecological Simulation System (RHESSys) that represents these ecosystem characteristics in a hydrologic modeling system.

Historically, hydrologists treated the vegetation on watersheds as passive wicklike evaporating surfaces, and calculated evapotranspiration as the residual of precipitation input minus measured streamflow, often computed at only monthly to annual intervals. Once an ET fraction had been established, a simple mass balance computation was applied to predict discharge for a watershed. For example, streamflow records were measured for a 185-km^2 watershed in Montana with annual precipitation of 152 cm and annual discharge of 109 cm giving a ratio of annual ET to precipitation of 0.28, or a runoff ratio of 72% (Running *et al.*, 1989). The RHESSys-modeled annual ET/precipitation ratio ranged from 0.26 to 0.32 for the different hill slopes of the watershed, producing both daily estimates and georeferenced spatial heterogeneity that simple mass balance approaches cannot provide.

Stream discharge is a particularly important variable for regional modeling as it is one of the few spatially integrated variables with direct validation data and documentation, namely, stream hydrograph records. Band *et al.* (1993) simulated peak seasonal stream discharge from the 15-km^2 Soup Creek watershed in Montana with an accuracy within 10 days of observations using RHESSys. White and Running (1994) expanded the approach to simulate daily discharge of the 2922-km^2 Middle Fork of the Flathead River of Montana, a mountainous region with evergreen forests, ranging from 1000 to 3000 m elevation and experiencing a range in precipitation from 750 to 1400 mm $year^{-1}$. River discharge varies from 0.6 mm day^{-1} in February to 8.6 mm day^{-1} in June. Spring snowmelt provides 78% of annual stream discharge during the April–July melt season. White and Running (1994), using RHESSys, simulated river discharge with a correlation of $r^2 = 0.80$ between predicted and observed daily values. Wigmosta *et al.* (1994) built a similar modeling system with strongly coupled hydrologic and ecological processes, and tested it on the Middle Fork of the Flathead River basin. The predictions of daily river discharge produced an r^2 of 0.91 with observed values, and the estimates of total annual runoff were within 7% of that measured. In these studies, evapotranspiration, photo-synthesis, dynamics of canopy water potentials, and other ecosystem processes were simulated by the mechanistic hydroecological models, but only stream discharge can be directly validated against daily measurements.

With RHESSys we can explore the hydrologic consequences of various landscape-level ecological disturbances that may have occurred in the past, be operating now, or be

projected for the future. A longtime retrospective analysis was completed by Pierce *et al.* (1993) to evaluate the influence of historic land-use change on regional hydrology of the 1 million km^2 Murray–Darling basin in Australia from pre-European settlement times to the present. Increased localized salinization and waterlogging of soils were hypothesized to be the result of widespread forest clearing, with an estimated 12–15 billion trees removed since the 1700s (Walker *et al.*, 1993). RHESSys simulations for a selected sample area of 7750 km^2 suggested that ET has decreased by 10–45 mm month^{-1} in the Murray–Darling basin as a consequence of deforestation. The areas of largest hydrologic surplus, predominantly riparian valley bottoms, are now being considered for reforestation (Fig. 8.6).

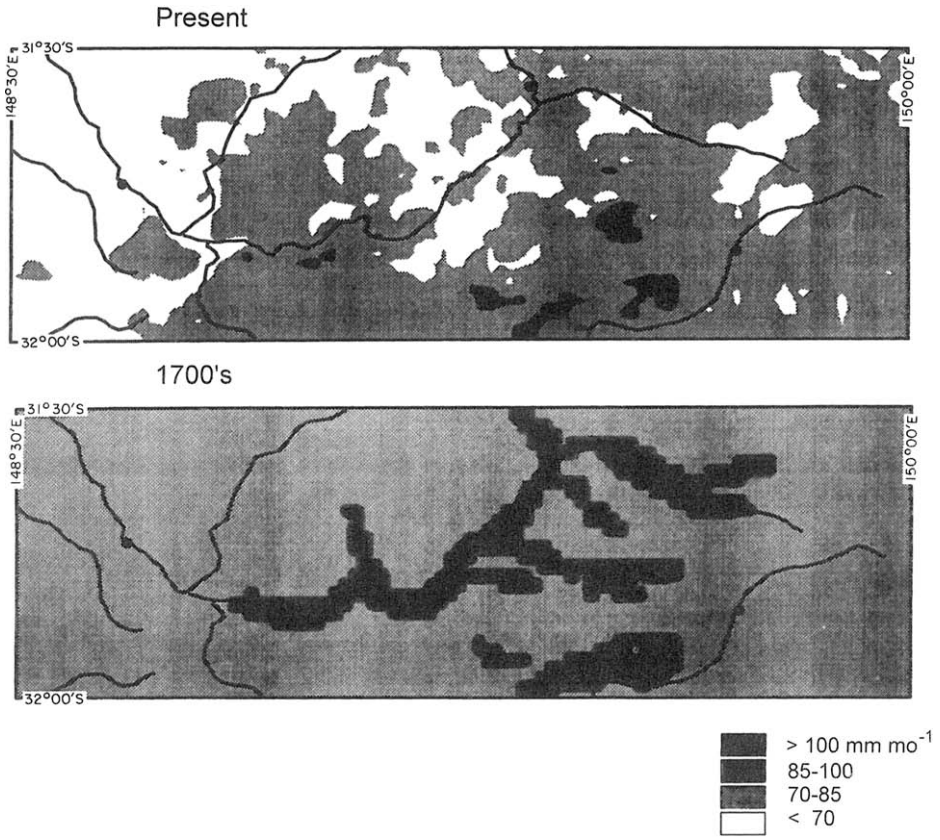

FIGURE 8.6. RHESSys simulation of the change in evapotranspiration within a 7750-km^2 study area of the 1×10^6 km^2 Murray–Darling basin of Australia. European settlement of the region 200 years ago replaced the native eucalyptus and acacia woodlands with farmland and pastureland, which greatly reduced evapotranspiration and increased the areas with waterlogged and saline soils. This simulation identified areas planned for tree planting to increase ET, which are predominantly riparian areas situated along the river networks. (Redrawn from Pierce *et al.*, 1993.)

As we think of a landscape in a more integrated and dynamic sense, we want to be able to predict what will happen to streamflow if portions of a watershed are harvested, burned, or planted with nonnative (exotic) tree species. Simulations of the Onion Creek experimental watershed in California predicted how seasonal stream discharge would react to partial cutting of various fractions of the watershed, as well as to complete harvest. The input data layers required by RHESSys (Fig. 8.7) show the topographic partitioning,

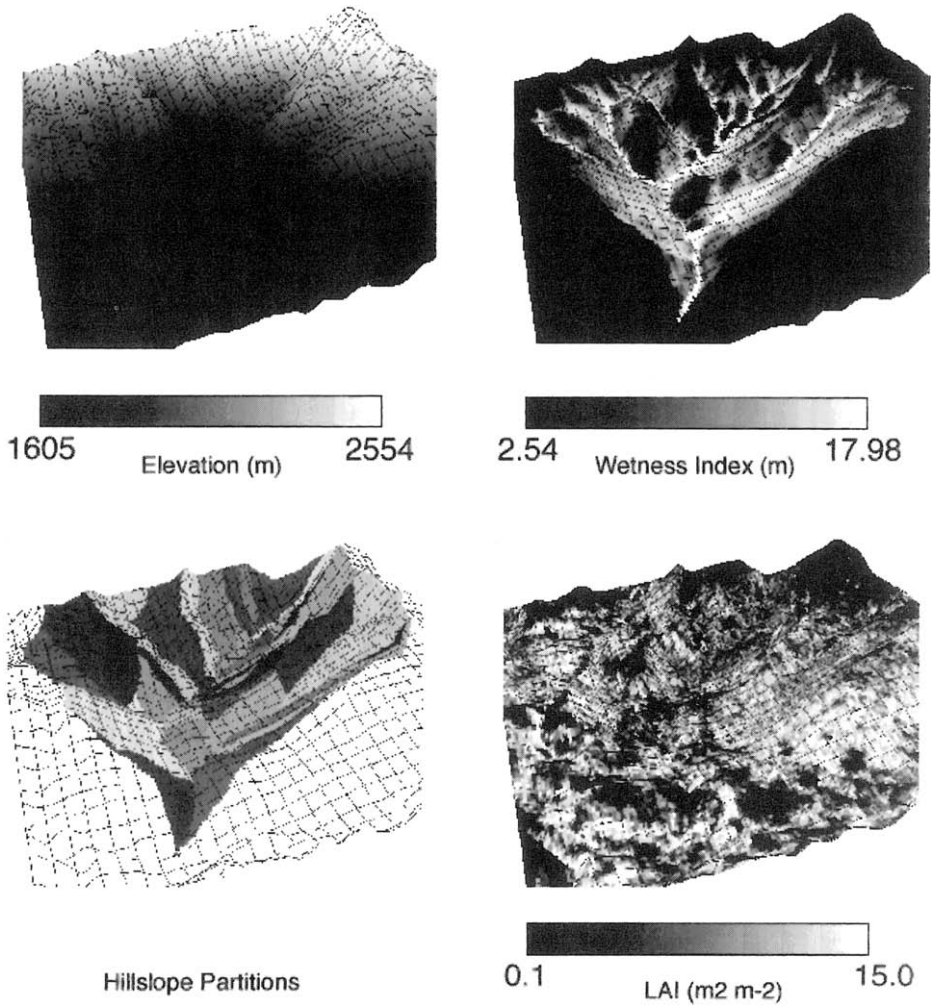

FIGURE 8.7. Topographic, soils, and vegetation data layers developed for the RHESSys simulation in Fig. 8.8 of the 25-km^2 Onion Creek watershed in the Sierra Mountains of California. The hill slope partitioning was based on algorithms developed by Band (1989a, 1993) to define landscape units with similar slopes, aspects, and elevations. The wetness index, based on the TOPMODEL logic of Beven and Kirkby (1979), represents the drainage capacity of different locations on the landscape. Leaf area index is calculated from Landsat TM data. (By R. Nemani, University of Montana.)

hydrologic drainage network, and current LAI of the watershed. Simulations with 100, 50, and 0% forest cover (Fig. 8.8) illustrated little sensitivity of wintertime ET and snowmelt processes to changes in forest cover. Growing season ET was proportionally reduced, and soil moisture (depicted as percent field capacity in Fig. 8.8) increased with reduction in forest cover. Forest removal was predicted to produce outflow events around year days 20, 50, 250, 300, and 350 that would not occur if full forest cover was maintained. Peak outflow increased from 12 to 18 mm day^{-1} and could contribute to downstream flooding. Whether this enhanced outflow would be beneficial for downstream irrigation or might cause flooding can only be answered in a broader regional hydrologic analysis. However, the predictive capability of these process-based hydroecological models can provide managers an understanding of the present state of landscapes on streamflow and encourage study of alternatives to minimize the possibility of implementing undesirable policies.

Many hydrology studies have illustrated that streamflows temporarily increase after extensive forest harvesting in a watershed, due to reduced ET (Bosch and Hewlett, 1982). The time required for streamflows to return to normal is termed *hydrologic recovery* and has been assumed to be anywhere from 30 to 100 years, depending on the climate and

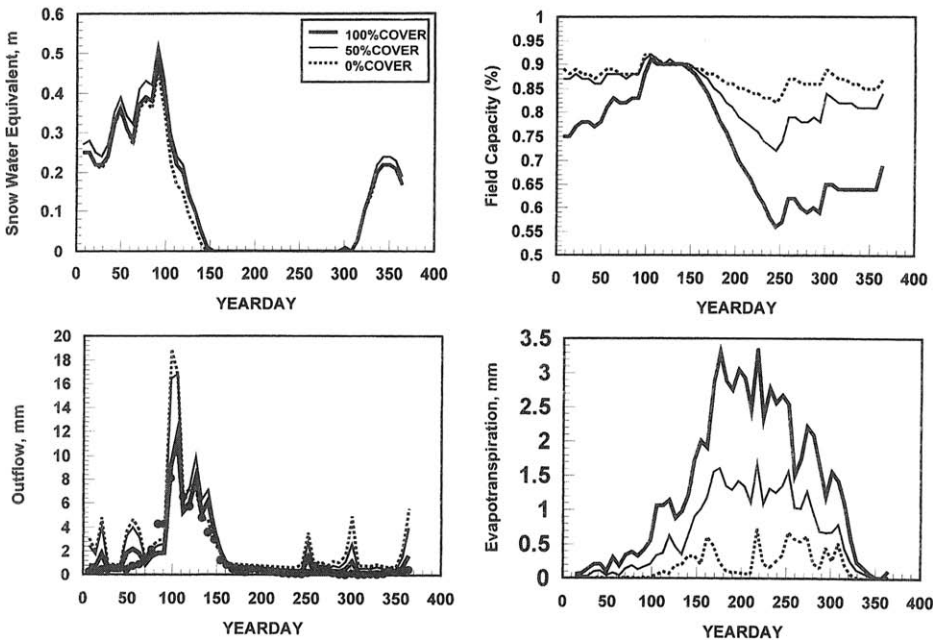

FIGURE 8.8. RHESSys simulation of the 25-km^2 Onion Creek watershed in the Sierra Mountains of California, using the data layers from Fig. 8.7. This simulation explores the potential consequences to the hydrologic budget of clear-cutting various fractions of the watershed, including estimates of seasonal peak outflow that could cause flooding. Points on the outflow graph represent measured daily stream discharge with the current 100% forest cover. Simulation tools such as RHESSys provide managers the ability to evaluate consequences of land management before any forest harvesting might be done. RHESSys can simulate different spatial patterns or temporal sequences of cutting, and check resulting potential streamflow responses for flooding during wet years or minimum flows during dry years. (By R. Nemani, University of Montana.)

postharvest recovery dynamics of the local forests (also see Chapter 2). Analyses with RHESSys have suggested that the true period of hydrologic recovery, generally corresponding to when the transpiring leaf area of the landscape has returned to preharvest conditions, may be much shorter (5–20 years), which could alleviate some management constraints on watersheds. For example, McKay and Band (1997) simulated a clear-cut in the Turkey Lakes watershed of Ontario by reducing the LAI from 7 to 1.5. Annual hydrologic discharge increased from 825 to 980 mm the year after clear-cutting. However, RHESSys simulated recovery of LAI to 7 within 10 years, at which point annual discharge returned to preharvest values (Fig. 8.9). Stem biomass recovery is not mechanistically related to hydrologic dynamics (and required >50 years for regrowth in this study), but it is often inappropriately used as the field measure of stand development for hydrologic recovery.

On longer time horizons, how would climatic change impact streamflows? Running and Nemani (1991) predicted the hydrologic consequences of a future climate change scenario of doubled CO_2, increasing air temperature by 4°C and precipitation by 10%, on Montana watersheds. Simulations suggested that snowpack, the source of most streamflow in the Rocky Mountains, would melt 19–69 days earlier in the spring, depending on topographic location. Average summer streamflows, however, would *decrease* by as much as 30% from current discharge levels, a change in hydrologic activity equivalent to the extreme drought year of 1988 in the western United States when some smaller rivers ceased flow by late summer for the first time in memory. Ironically, these RHESSys simulations showed forest productivity to be enhanced by the climate change scenario, partially because of the direct CO_2 response of photosynthesis and partly because of the longer growing season and higher soil water availability brought on by earlier snowmelt. Clearly, projecting regional ecosystem responses to interannual climatic variability or to more permanent changes requires a consideration of hydrologic and ecological interactions that may not be immediately obvious.

B. Watershed Biogeochemistry

Analysis of the biogeochemistry of a watershed requires not only a good hydrologic balance model as transport medium, but also good models of precipitation inputs, soil elemental cycling, and mobility (Aber *et al.*, 1993). Ollinger *et al.* (1993) built a model of atmospheric elemental deposition for the northeastern United States. Observations of precipitation were extrapolated to mountainous areas with elevational relationships similar to those discussed in Chapter 7. Elemental concentrations of nitrogen, sulfur, calcium, and potassium species were measured in the U.S. National Atmospheric Deposition Program. Spatial maps of elemental input were then produced by relating measured elemental concentrations with the precipitation of each landscape element, and summarizing these predictions into maps extending across the 11-state region.

Integrating watershed biogeochemistry with hydrology requires adding a mechanistic terrestrial nutrient budget to the model analysis. Creed *et al.* (1996) coupled the nitrogen budget of FOREST-BGC with RHESSys to calculate the seasonal dynamics of nitrate export from the Turkey Lakes watershed in Ontario, Canada. Creed *et al.* (1996) identified two mechanisms for seasonal nitrogen release (Fig. 8.10). The first is an N-flushing

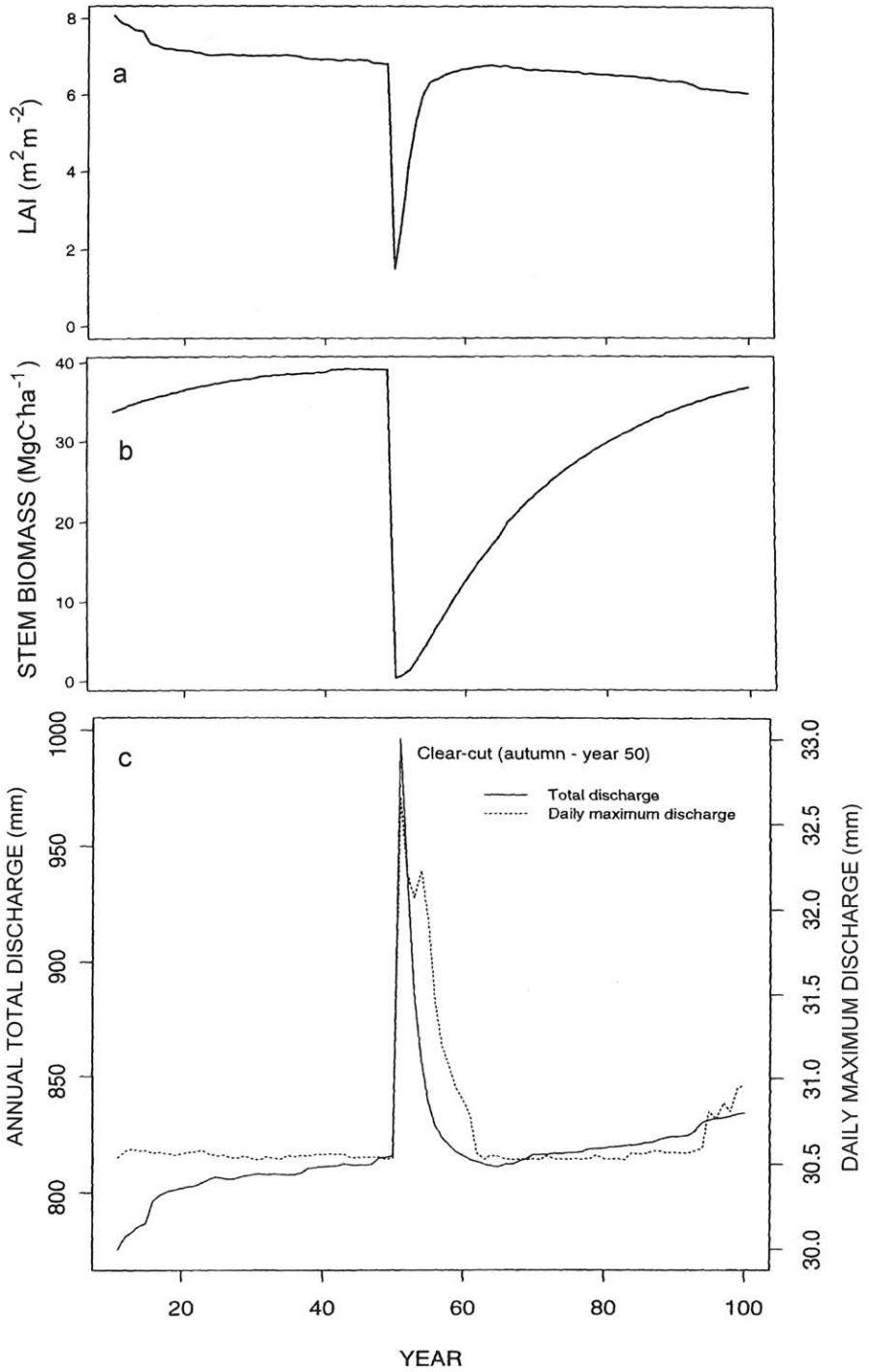
a
LAI ($m^2 m^{-2}$)
0
2
4
6
8
b
STEM BIOMASS ($MgC ha^{-1}$)
0
10
20
30
40
c
Clear-cut (autumn - year 50)
Total discharge
Daily maximum discharge
ANNUAL TOTAL DISCHARGE (mm)
800
850
900
950
1000
DAILY MAXIMUM DISCHARGE (mm)
30.0
30.5
31.0
31.5
32.0
32.5
33.0
20
40
60
80
100
YEAR

mechanism associated with snowmelt when soils become saturated. After a period of low N demand by forests during the winter, soil N enrichment occurs, so that saturated flows export large amounts of N in the spring. Second, during nonsaturated flow conditions, an N-draining mechanism transfers mobile N to lower soil horizons below the tree rooting zone, where continuous hydrologic base flow slowly releases N throughout the year. Removal of forest cover eliminates canopy interception and reduces uptake from the rooting zone, which accelerate N release from a watershed until the forest canopy is reestablished.

Elements can be transported in solution or in suspended sediments. The concentrations of these elements are a prime determinant of water quality. Hunsaker and Levine (1995) emphasized the necessity of accurately characterizing the entire land cover and land-use pattern of a watershed to represent elemental mass balances and their seasonal dynamics. The analysis confirmed the necessity of including the elemental contributions of land units well beyond the immediate proximity of the riparian zone.

C. Landscape Carbon Balances

Sustainable yield, whether of wood products or domestic and wildlife forage, is ultimately related to the net primary productivity of the landscape. Although our understanding of the components of an ecosystem carbon budget were well developed in Chapter 3, the implementation of that knowledge across a landscape is complicated by varying microclimates, soils, and stand conditions. Running *et al.* (1989) first used an early version of RESSys without hydrologic routing to simulate annual photosynthesis of the 1200-km^2 Seeley–Swan basin of Montana. The net photosynthesis computed across this complex mountainous landscape ranged from 9 to 20 Mg C ha^{-1} year^{-1}; however, CO_2 fluxes cannot be directly validated by observations. Our confidence in these regional calculations is based on comparisons of FOREST-BGC predictions against stand-level measurements (McLeod and Running, 1988; Korol *et al.*, 1991; Running, 1994). Because the early RESSys incorporated no hydrologic routing, these simulations are an example of an unconnected landscape analysis, that is, each cell was computed with complete independence from adjacent cells. Band *et al.* (1993) and White and Running (1994) incorporated the hydrologic routing of RHESSys into landscape simulations of photosynthesis and NPP. Carbon balances were improved at the bottom of hill slopes where water was received from lateral flow draining from above. This source of seepage water alleviated summer water stress and enhanced annual photosynthesis and NPP of the riparian vegetation.

The degree of complexity represented in a landscape simulation can influence the results. White and Running (1994) simulated annual NPP on the 414-km^2 McDonald

---

FIGURE 8.9. A 100-year RHESSys simulation of the 10-km^2 Turkey Lakes watershed in Ontario, Canada, explored the rate of hydrologic recovery after simulating a clear-cut of the native sugar maple forest at year 50 (McKay and Band, 1997). Although stem biomass did not return to precut levels for 50 years, LAI recovered within 10 years, causing annual stream discharge to also recover at a similar rate. Return of peak daily discharge to original levels, the critical variable for flooding, was only slightly slower. See Band *et al.* (1993) for additional details on methods. (From McKay and Band, 1997, *Hydrological Processes* **11,** 1197–1217. Copyright John Wiley & Sons Limited. Reproduced with permission.)

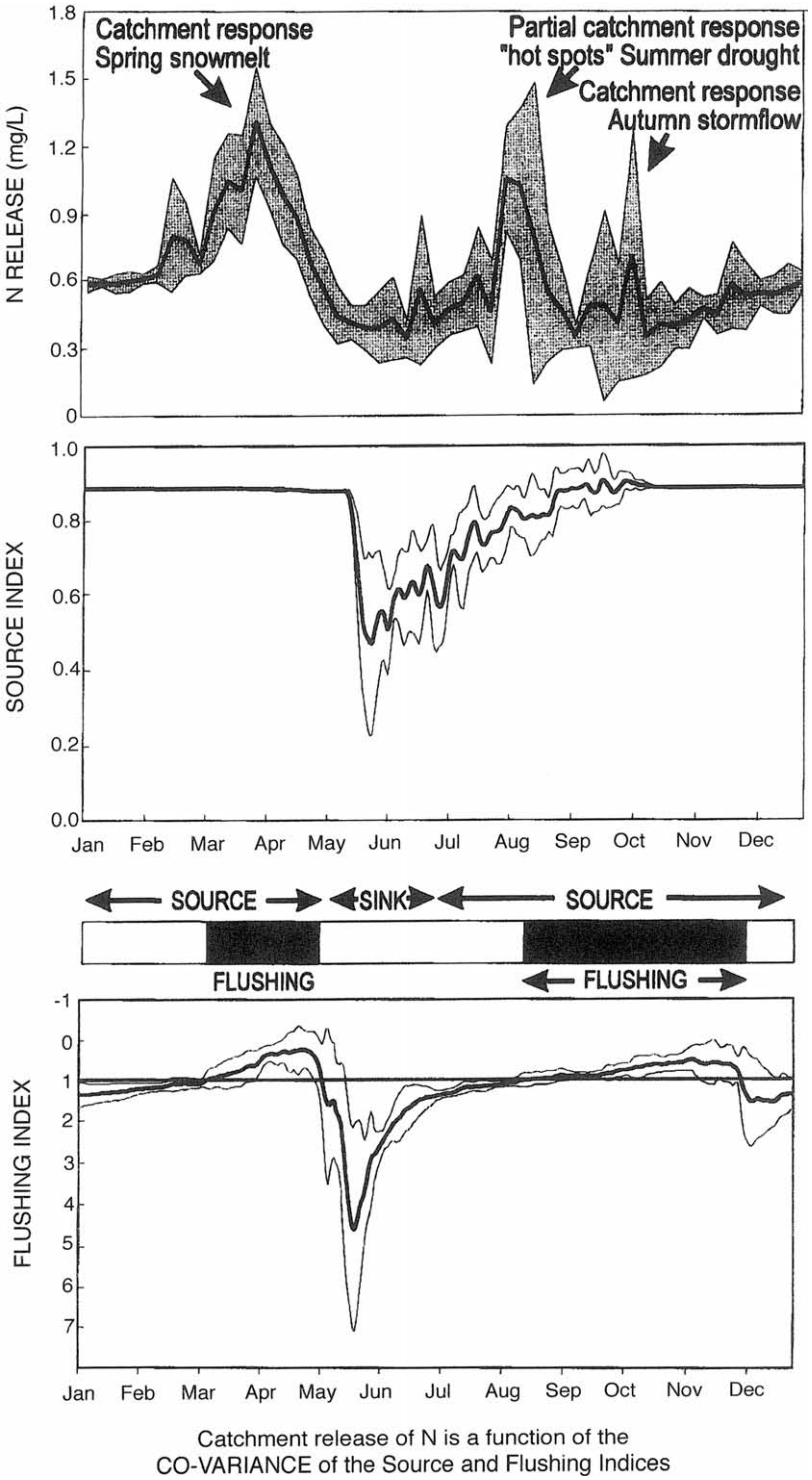

Catchment release of N is a function of the
CO-VARIANCE of the Source and Flushing Indices

watershed of Glacier National Park, Montana, using four techniques that progressively increased the detail defined on the landscape. The simplest landscape representation was unconnected 1-km raster (square) cells, and the most complex defined 855 hydrologically connected polygons in a RHESSys simulation. Final basin average NPP ranged from 7.04 to 7.55 Mg C ha^{-1} $year^{-1}$ with the four methods of calculation, but the within basin NPP ranged from 2.5 to 15.5 Mg C ha^{-1} $year^{-1}$, with highest productivity on the warm, lower south slopes and lower productivity on high, north slopes with shallow soils. White and Running concluded that for broad landscape averages the simplified satellite-driven NPP calculations based on the Light Use Efficiency model from Chapter 3 would be adequate, but for site-specific management decisions the full RHESSys modeling analysis including hill slope unit definition was recommended. Pierce and Running (1995) also evaluated potential errors propagated by landscape aggregation, and they found that overestimates as high as 30% were possible if NPP was computed from broad $1° \times 1°$ cell attributes, as done by global scale models, compared to 1-km cells based on AVHRR data. Rastetter *et al.* (1992) suggested a number of statistical tools for dealing with such landscape aggregation errors.

These geographically explicit simulations of forest NPP quantify both the heterogeneity of the landscape and the environmental factors that limit tree growth, so could serve as the basis for improved computation of sustainable harvest levels in managed forests. Although direct field measurements are still the best means of determining local forest growth rates, ecosystem models can more accurately extrapolate stand data to the rest of the landscape and offer the additional advantage of exploring landscape responses to alternative management options.

Milner *et al.* (1996) applied a simplified RESSys logic to simulate the potential NPP of private forested lands in Montana for purposes of defining tax rates. Productive *potential*, not current productivity, was sought as a reference by the state government to encourage more intensive management of the more productive forest lands. The biophysical principles incorporated in RESSys were appropriate for defining ecological potential and did not require extensive data of current stand conditions. The final map produced from the regional analysis illustrates five productivity classes ranging from <1.7 to >5.9 $m^3 ha^{-1}$ $year^{-1}$ of stem wood (see Plate 6). Because the evaluation is based on established ecological principles from Chapters 2–4, the introduction of different species, genetically improved trees, fertilization, climatic change, or other changes in the ecosystem could all be incorporated in a reevaluation if desired. Also, it was estimated that the statewide analysis of 14,200 km^2 of forested land was done by biophysical model analysis for a quarter of the cost and half the time that an intensive field inventory based method would have required.

FIGURE 8.10. RHESSys simulation of seasonal nitrate release in streamflow from the Turkey Lakes watershed in Ontario, Canada. Creed *et al.* (1996) hypothesize two mechanisms of nitrate release, an N-flushing dynamic during saturated soil conditions during spring snowmelt and autumn storm flow, and a second release during midsummer when mobile N has drained below the rooting zone and slowly enters into the groundwater. The source index defines the balance between the supply of available N from mineralization relative to the demand for N by plant uptake. The flushing index quantifies the availability of soil water as a mechanism for N transport. (From Creed *et al., Water Resources Research* **23,** 3337–3354, 1996, published by the American Geophysical Union.)

D. Regional Biogeochemical Applications

1. Glacier National Park

A multiresource analysis in Glacier National Park, Montana, that incorporated RHESSys modeling to link wildlife, hydrologic, and vegetation studies together was designed to obtain a wider range of analytical capability for land management. Site physical data on topography and soils, stand structural data, climatic measurements, and snow and stream dynamics were organized to provide input data layers for RHESSys, and output variables were selected for which validation data were available. The McDonald and St. Mary's drainages represent topographically, climatically, and ecologically diverse landscapes of two connected watersheds which cross the Continental Divide. Plate 2 illustrates how digital elevation data and soil physical data were incorporated in the TOPMODEL analysis to provide soil transmissivity and saturation indices for hydrologic routing in RHESSys, and soil water holding capacity, for initializing FOREST-BGC. Plate 7 shows the geographic location of the study area. An SR (Simple Ratio, Chapter 7) was computed from Landsat TM data, and a nonlinear transformation to LAI was made on the basis of field plot measurements throughout the study area (White *et al.*, 1997a). The forest community types were defined with a fuzzy logic classifier combining observed topographic relationships with Landsat spectral data in red, near-infrared, and mid-infrared wavelengths.

Eight-year RHESSys simulations of carbon and water balances were executed for the McDonald watershed applying the input data layers indicated in Plates 2 and 7, and selected variables were validated with field plot data (see Plate 8). Aboveground NPP was highest at low to mid-elevations on forests that had not been disturbed recently by wildfire or avalanches. High elevations and north slopes were more energy limited and typically had shallow soils and slow snowmelt, conditions that restrict the growing season. A growth efficiency map, defined from the principles in Chapter 5, clearly separated the oldest stands, with lowest wood production/LAI, from the younger stands with higher efficiency. This map could serve to delineate areas with high hazard rating that are particularly susceptible to mountain pine beetle outbreaks. The inserted validation graphs present observed and modeled 8-year stem growth increments, translated into NPP units. All plots measured in the drainage had highest NPP in 1987 as a result of warmer than average temperatures and average precipitation for that year.

The annual snowpack map (Plate 8) shows the areas of highest snow accumulation, and the inset validation graphs show predicted versus observed monthly snow water equivalents from snow course survey data. The northern Rocky Mountains have a strong snowmelt-dominated seasonal hydrology, illustrated by the peak stream discharge around year day 140 and near minimal discharge from year days 1–80 and 280–365 when temperatures are nearly continuously below freezing. The persistent underestimate of simulated stream discharge may be a result of contributions from melting glaciers in the upper reaches of the watershed that were not accounted for by RHESSys.

In Chapters 5 and 6 we learned that projecting a forest forward in time over centuries requires analysis of forest processes in stand development, community dynamics, and disturbance activity. In Chapter 6 we introduced a model that combined the ecophysiology of FOREST-BGC with the stand dynamics and disturbance timing of a gap model,

FIRE-BGC (Keane *et al.*, 1996a,b). The stand-level FIRE-BGC model was embedded in a spatial modeling framework that simulates probability of ignition on the basis of historic fire frequency, fire behavior and spread rates associated with fuel loading, topography, and microclimate, and tree mortality, with mortality being computed from simulations of fire intensity and duration. Seed dispersal was then computed as a probability to estimate the species composition and spatial distribution across the regenerating landscape.

With this multifaceted modeling system we can now ask real-world land management questions, such as what might the Glacier National Park landscape look like 250 years from now as climate changes, and how will fire management policy influence that result? Furthermore, how will the landscape differ if a complete fire suppression and exclusion policy is practiced, as has predominated for the last century, or if managers allow a more natural fire frequency to return for the next 250 years? These important questions are made more difficult to answer because the natural fire frequencies measured in the field by analyzing fire scars are based on historic climate. What would a new natural fire frequency be in a different climate, and how would fire intensity, a highly climate-sensitive variable, change? Keane *et al.* (1997) attempted to answer these kinds of questions by simulating fire and ecosystem responses for the same Glacier National Park landscape depicted in Plate 7 for 250 years first with historical climate and full fire suppression, then with a potential future climate and the resulting natural fire frequency. The current climate for these simulations was defined from 44 years of measured weather data replicated for a 250-year simulation with topographic microclimate variability, including humidity and solar radiation computed from MT-CLIM (see Chapter 7). A climate change scenario was evaluated, based on global circulation model predictions for the twenty-first century that would increase air temperatures by 2°–5°C and precipitation by 25–30%, with a doubling of atmospheric CO_2 levels.

The number of fire ignitions were predicted to not change with the future climate, but fire intensities were predicted to triple and the extent of burning to double under the future climate, with some areas being burnt up to 7 times in 250 years (see Plate 9). This dramatic change in fire dynamics resulted because of higher NPP and forest encroachment into areas that were meadows. The increased accumulation and more contiguous distribution of fuels allowed fires, once started, to burn more intensely over wider areas. The rather complicated interactions and their implications could not be foreseen without comprehensive simulation modeling. Although we cannot confirm these simulations 250 years into the future, the results, once presented, seem reasonable, based on our understanding of this system and the detailed information provided in the multidimensional analysis.

2. Columbia River Basin

The 820,000-km^2 interior Columbia River basin of the Pacific Northwest, which encompasses parts of eight states, was chosen in 1993 to be the test bed for developing ecosystem management principles for federal land managers in the western United States. The Columbia basin is hydrologically the most important river drainage in the northwestern United States in terms of hydroelectric and irrigation activity, and it encompasses ecological diversity from some of the most productive forests to one of the most desolate deserts in the United States. At this broad regional scale, the management questions were as

follows: What is the primary productivity of this region; has it changed in the last century with increased exploitation and management, and is current productivity *sustainable*? What risks of accelerated ecosystem disturbance are likely from insect, disease, or fire activity that may influence sustainable productivity? How do land managers balance the multiple interests of hydrologic needs for irrigation, hydroelectric power, and anadromous fish habitat?

A RHESSys simulation of daily carbon and water balances was executed at 2 km spatial resolution for the entire basin. To evaluate interannual variability, 3 years of weather station records were selected for the simulations: 1982, 1988, and 1989, representing a cool-wet, hot-dry, and average year climatically. The DAYMET model, a spatial version of MT-CLIM, provided extrapolation of climate data for the entire basin (Plate 3; Thornton and Running, 1996). Both current and historical land cover of all biome types including forests, shrub lands, grasslands, and crops were defined, to analyze changing productivity resulting from land-use conversions. Forest stand ages, species mixes, density, and structure were estimated for each cell from permanent plot records. We must recognize, however, that 205,213 cells were defined for this regional simulation, so parameter values are based on relationships defined among variables and automatically assigned to a cell; each cell could not be individually considered.

The annual carbon budget for this region (see Plate 10) shows great seasonal variation in photosynthesis and respiration resulting from the cold temperatures and short day length of the winter season contrasting with strong activity in the early spring. The mid-growing season period of July and August represents the time of highest temperatures and maintenance respiration, but not the time of highest photosynthesis, because water stress and low humidity limit stomatal responses and canopy gas exchange (Chapters 2 and 3). Many of the areas of highest gross photosynthesis (dense forests of high LAI) also have high maintenance respiration, so the final annual net photosynthesis (and NPP) is rather similar across biome types in similar climatic zones. The difference between NPP of the historic and current landscape was not great, as NPP is controlled more by climatic regime than the vegetation type unless a site has been severely and recently disturbed. Annual NPP was 8% higher in the cool-wet year of 1982 and 37% lower in the hot-dry year of 1988, compared to the normal year 1989 shown in Plate 10.

This analysis documents that the dominant factor controlling photosynthesis and productivity in this region is water more commonly than energy, except for cooler, wetter sites in the high mountains where temperature limits the growing season. The carbon balance simulations were summarized into a carbon stress index, the ratio of maintenance respiration to gross photosynthesis, as a simple measure of carbon availability for plant growth and defense. This carbon stress index, which is the regional equivalent of the stand-level growth efficiency index, identifies forests most susceptible to insect/disease attack (Chapter 6). Older stands on drier sites, with high respiration costs but water-limited photosynthesis, had highest carbon stress indices, and hot-dry years such as 1988 accentuated stress by both raising respiration and lowering photosynthesis. Grasslands and shrub lands tend to have low carbon stress indices as a result of less investment in respiring tissue.

The seasonal hydrologic dynamics of the Columbia basin are clearly dominated by spring snowmelt (see Plate 11). Although precipitation is fairly evenly distributed

seasonally, it is accumulated as snowpack from November to February, snowmelt and hydrologic outflow are concentrated in the period March to May, and virtually no outflow occurs from July through October, except from the high mountain watersheds. Daily evapotranspiration far exceeded precipitation during the early growing season until stomatal restrictions limited ET in July and August. Soil moisture was depleted from April to August, with some autumn recharge before snow began to accumulate (Chapter 2). Most of this region could not support cropland without reservoirs for water storage and irrigation during the summer period, but anadromous fish migration requires late summer water flow in the lower Columbia River which causes a conflict with demands for irrigation water. Average basin river outflow was 38% higher during the cool-wet year 1982, and 20% lower during the hot-dry 1988 year than the normal 1989 climate year shown in Plate 11.

It is evident that analysis of an 820,000-km^2 region can only provide information useful for defining broad policy objectives and should not be used for management of specific sites. The key criteria for whether a regional model analysis can support detailed versus only general interpretations lies in the accuracy with which landscape variables were assigned to individual cells. The assumptions, generalities, and inaccuracies involved in defining site and stand parameters for hundreds of thousands of cells for this simulation reduces accuracy at the local level. Although it may be simple to define the stem biomass for a stand-level simulation of FOREST-BGC from plot inventory data, we lack procedures or data to assign accurate stem biomass for 820,000 km^2. Nevertheless, some valuable analyses are possible. Where are the most and least productive landscapes in the region? How much irrigation water or hydroelectric production may be possible in a record drought year? Where are the most logical areas for irrigated agriculture, intensive forest management, and other land-use alternatives? For example, NPP of forested land in the Columbia basin simulated in Plate 10 could be translated into the sustainable harvest, or "annual allowable cut," of wood products for the region. Details of where the harvest should take place would require more precise watershed scale simulations using field inventory data. The basic principle operating here is that the final accuracy obtained is less a function of the model's formulation than it is of the accuracy with which parameters are defined for the simulations. Planning and management of specific areas are usually more appropriately accomplished at the scales represented in Plates 7–9 because field data for points throughout the watershed can be used to initiate the models and obtain more accurate simulations.

E. Validating Regional Biogeochemical Models

We now have the capability to calculate regional biogeochemistry over millions of square kilometers; however, there are very few large-scale data sources for validating these simulations. Although a wealth of plot-level data is available for small-scale validation tests, as discussed in Chapters 2–6, validation activity specifically designed for large areas is rare. The most commonly available regional scale validation data are stream discharge records from which ET can be computed by mass balance and predictions of stream discharge can be compared, as presented in Figs. 8.7 and 8.8 and Plates 7 and 10. Over scales of a few kilometers, tower-based measurements of micrometeorological fluxes of energy, water vapor, and CO_2 can record diurnal to seasonal changes in forest fluxes (Baldocchi

et al., 1988; Desjardins *et al.*, 1992a,b). At larger scales, aircraft mounted with fast response gas analyzers can detect varying flux patterns across a landscape (Matson and Harriss, 1988; Sellers *et al.*, 1992a,b). Ray Desjardins (personal communication, 1996) showed high correlation between a radiometric vegetation index and aircraft-measured CO_2 flux rates across a 500-km transect of the Canadian boreal forest (Fig. 8.11). At still larger scales, the global atmospheric CO_2 station data can be used together with a transport model for terrestrial process validation, and will be covered in Chapter 9 (Hunt *et al.*, 1996). This difficulty of large-scale validation reemphasizes the importance of doing regional analysis with ecosystem models that have been tested at the stand level where the principles of ecosystem operation are well understood and model results can be compared directly against field measurements.

V. SUMMARY

Analysis of forest ecosystem processes is now possible at regional scales by integrating stand-level models with georeferenced databases. Remote sensing is an essential element of regional ecosystem analysis, as it provides complete and consistent measures of the landscape, but only for certain variables that can be measured with this technology. Satellites provide landscape maps of biome type and LAI, as well as regular monitoring of key

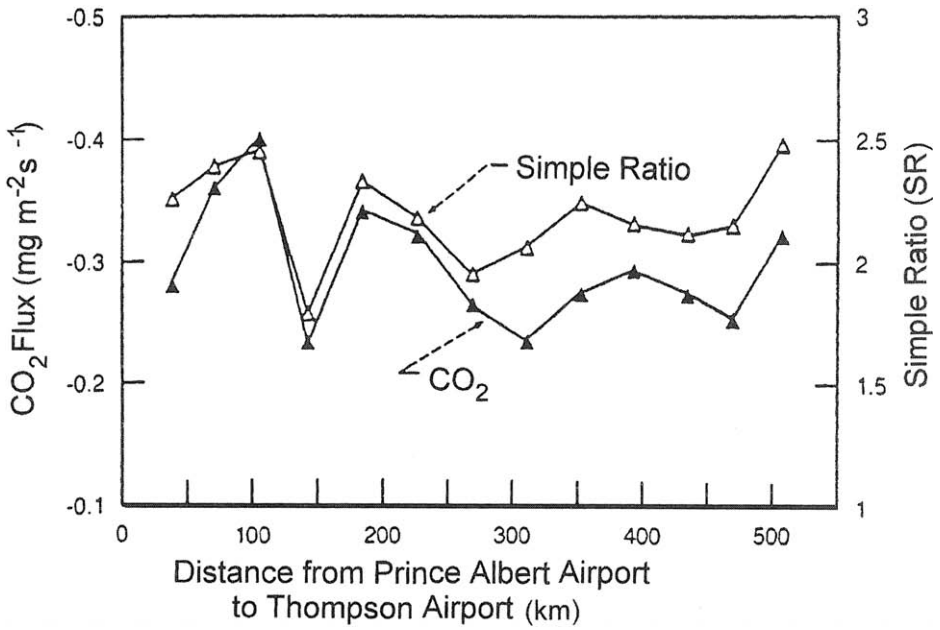

FIGURE 8.11. Regional scale measure of forest CO_2 flux measured by low-flying aircraft, compared to the Simple Ratio of NIR/Red remote sensing reflectance. The SR here is proportional to the land surface vegetation density (see Chapter 7). The BOREAS study area is in central Canada. Satellite, aircraft, and tower-based measurements will be required to provide validations for regional scale ecosystem simulations. (From Ray Desjardins, Agriculture Canada, personal communication, 1996.)

conditions such as drought and fire danger. Regional models simulate forest biogeochemical responses and stand dynamics at space and time scales relevant to land management. Predictions of wildlife population changes, recovery of hydrologic balance, and shifts in landscape productivity can now be simulated for a range of situations that include past, present, and an array of future conditions. As a result, alternative management policies can be evaluated before actions are implemented. Accurate georeferenced databases, however, are not yet generally available for many forested regions, which makes it difficult to initialize these integrated landscape models. Additionally, we lack ways of validating the current predictions of regional models because of the paucity of ecological data acquired at this scale, beyond that which can be obtained through remote sensing.

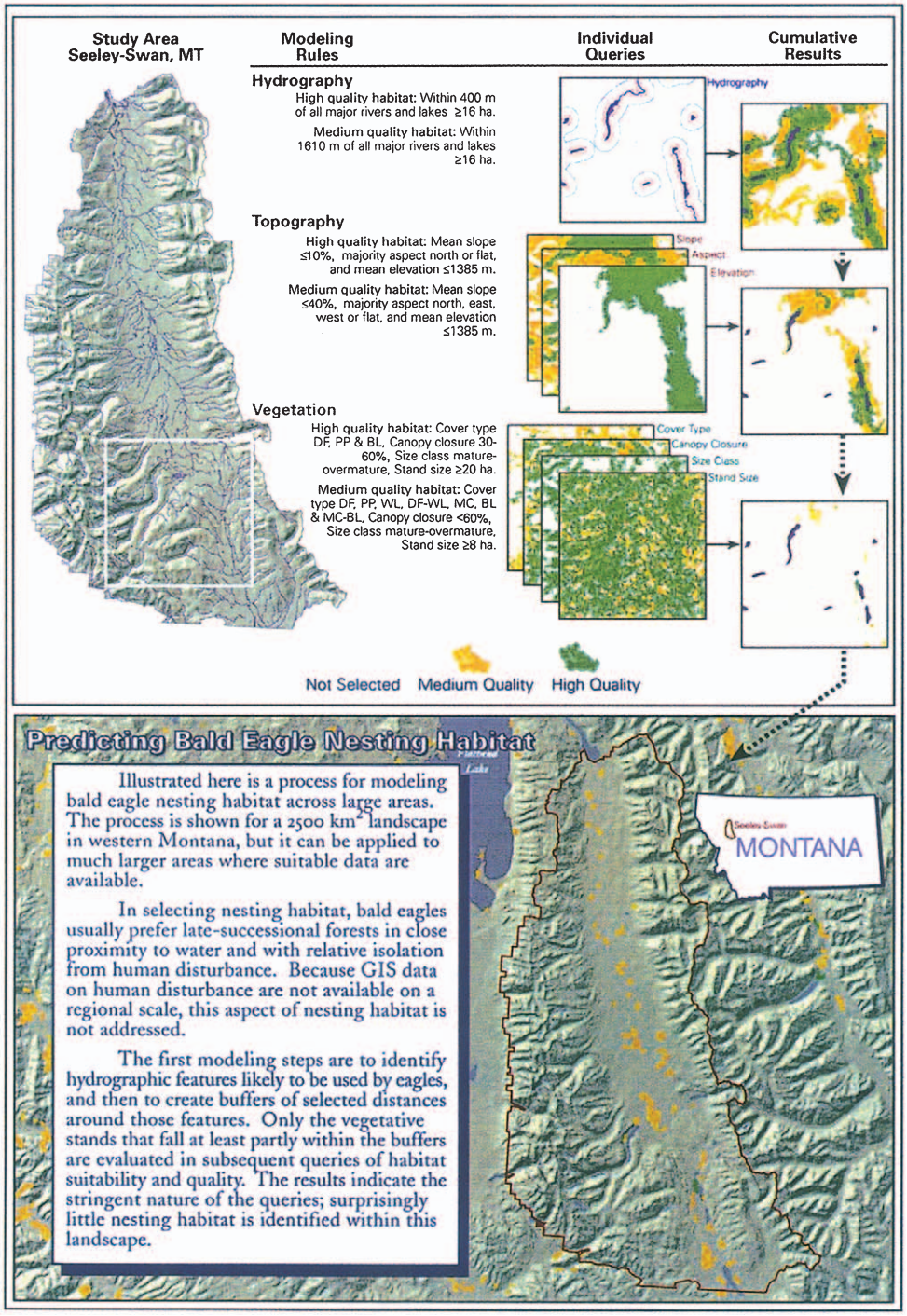

PLATE 4. Geographically explicit framework for modeling bald eagle habitat in a 2500-km^2 basin in Montana. Hydrography, topography, and vegetation data layers which define known species preferences (DF, Douglas-fir; PP, ponderosa pine; BL, broadleaf trees; WL, western larch; MC, mixed conifers) are merged with a logical hierarchy to reflect decreasing habitat priorities. The resulting analysis produces an intersection of required and optimum conditions. The habitat identified represents less than 1% of the study area and would warrant special management consideration. These procedures could be used for other species, but each will have different habitat requirements, necessitating somewhat different analysis. (From Steve Holloway and Melissa Hart, University of Montana Spatial Analysis Laboratory.)

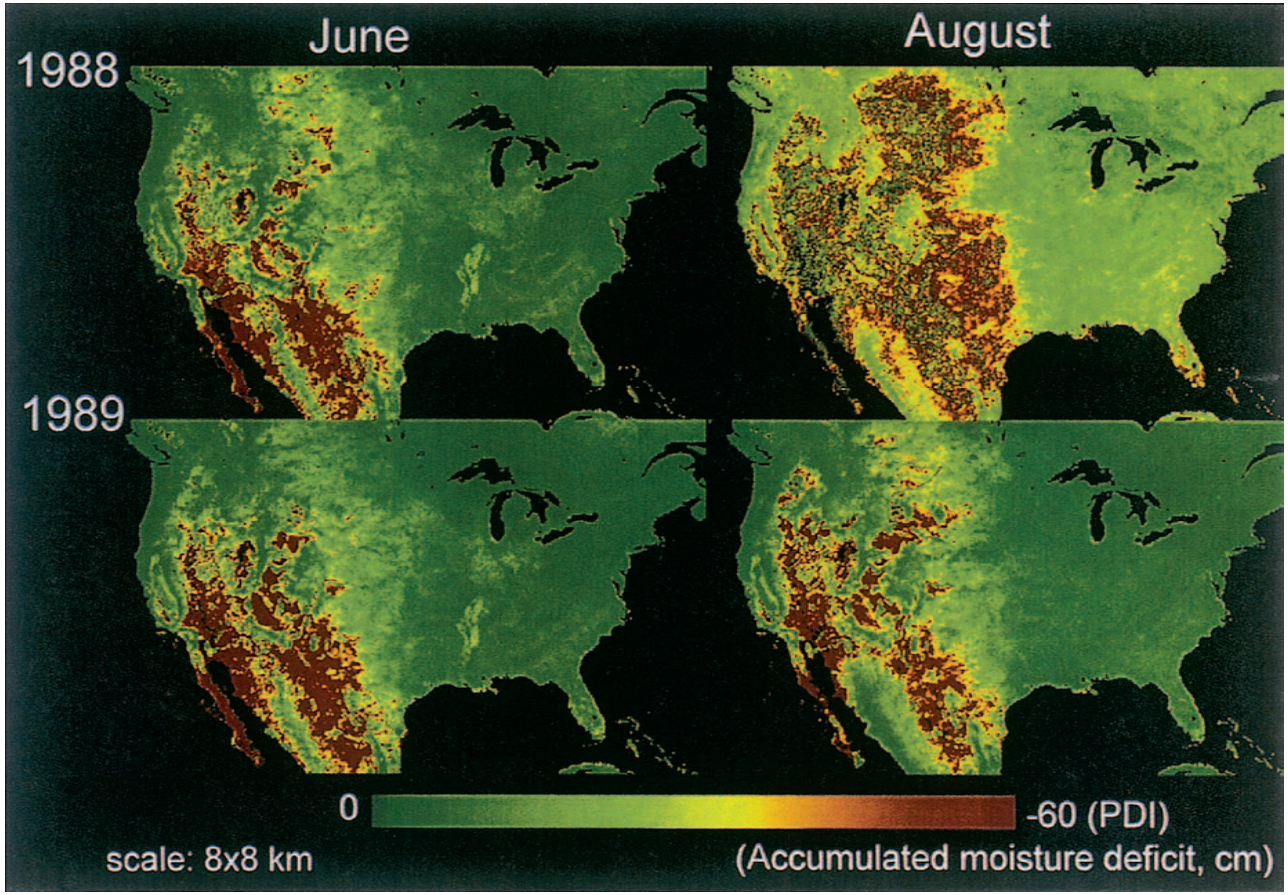

PLATE 5. Seasonal changes in a satellite-derived drought index produced from biweekly composited AVHRR NDVI values and radiometric surface temperatures for the United States, expressed as a moisture deficit similar to the Palmer Drought Index. The hot, dry conditions of the summer of 1988 which resulted in the huge Yellowstone National Park fires are clearly contrasted with the more normal conditions of 1989. This drought index can also be expressed as a fire danger index. Both indices are based on the T_s/NDVI relationship and surface resistance computation explained in Chapter 7 (Nemani and Running, 1989b; Nemani *et al.*, l993a). The Earth Observing System has produced a Drought Index weekly for the world since 2000.

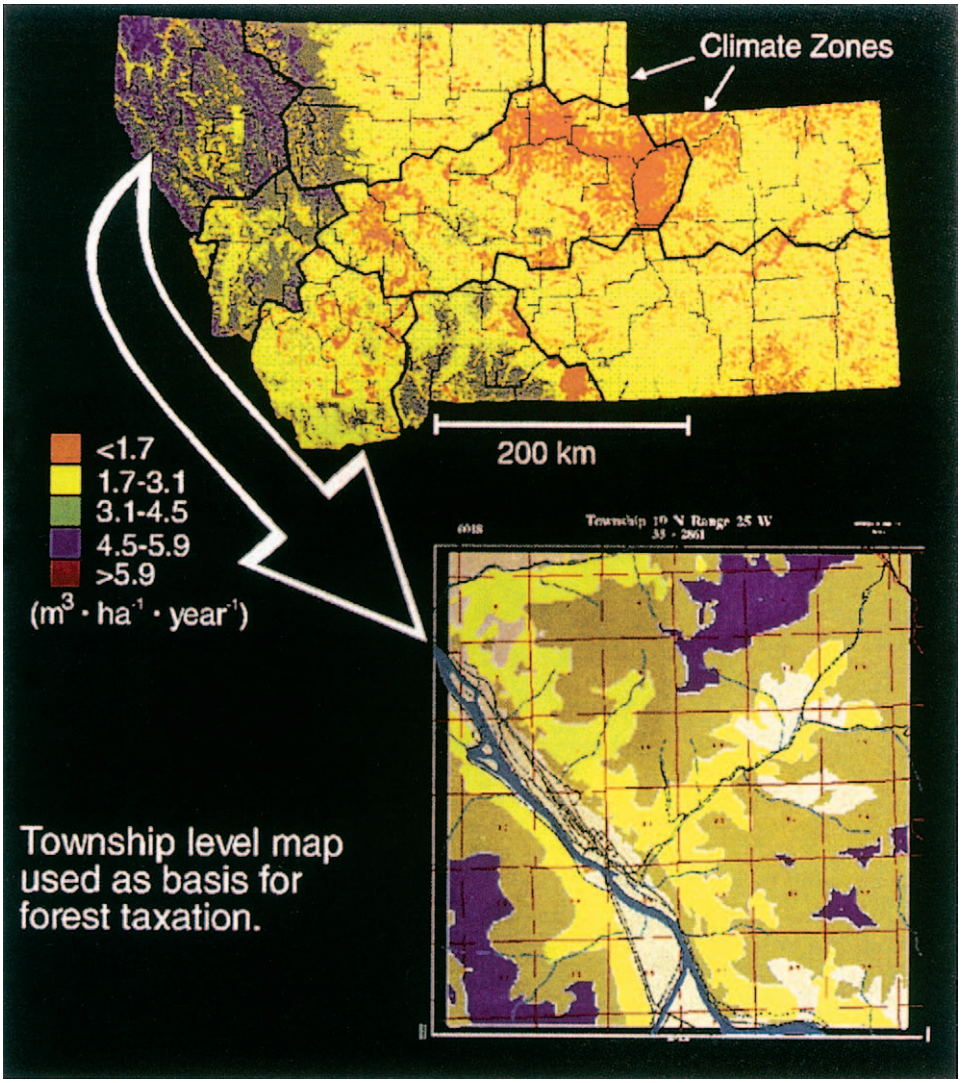

PLATE 6. Map of the potential forest productivity of Montana produced with RHESSys logic for the state forested land taxation system (Milner *et al.*, 1996). MT-CLIM was used to build a topographically sensitive daily climate data file. Potential LAI was computed from the hydrologic equilibrium concepts of Nemani and Running (1989a). Soil water holding capacities were computed from the STATSGO database. FOREST-BGC was then run with fixed physiological parameters representative of lodgepole pine. Rather than executing each of ~2 million cells individually, each climate/topography/LAI/soils combination was simulated and the appropriate result mapped back to each 0.36-ha cell. These computed productivities are now the basis of forestland valuation for property taxation in Montana. It was estimated that the model-based mapping was done for one-quarter of the cost and in half the time required for an equivalent field inventory. (From Milner *et al.*, 1996.)

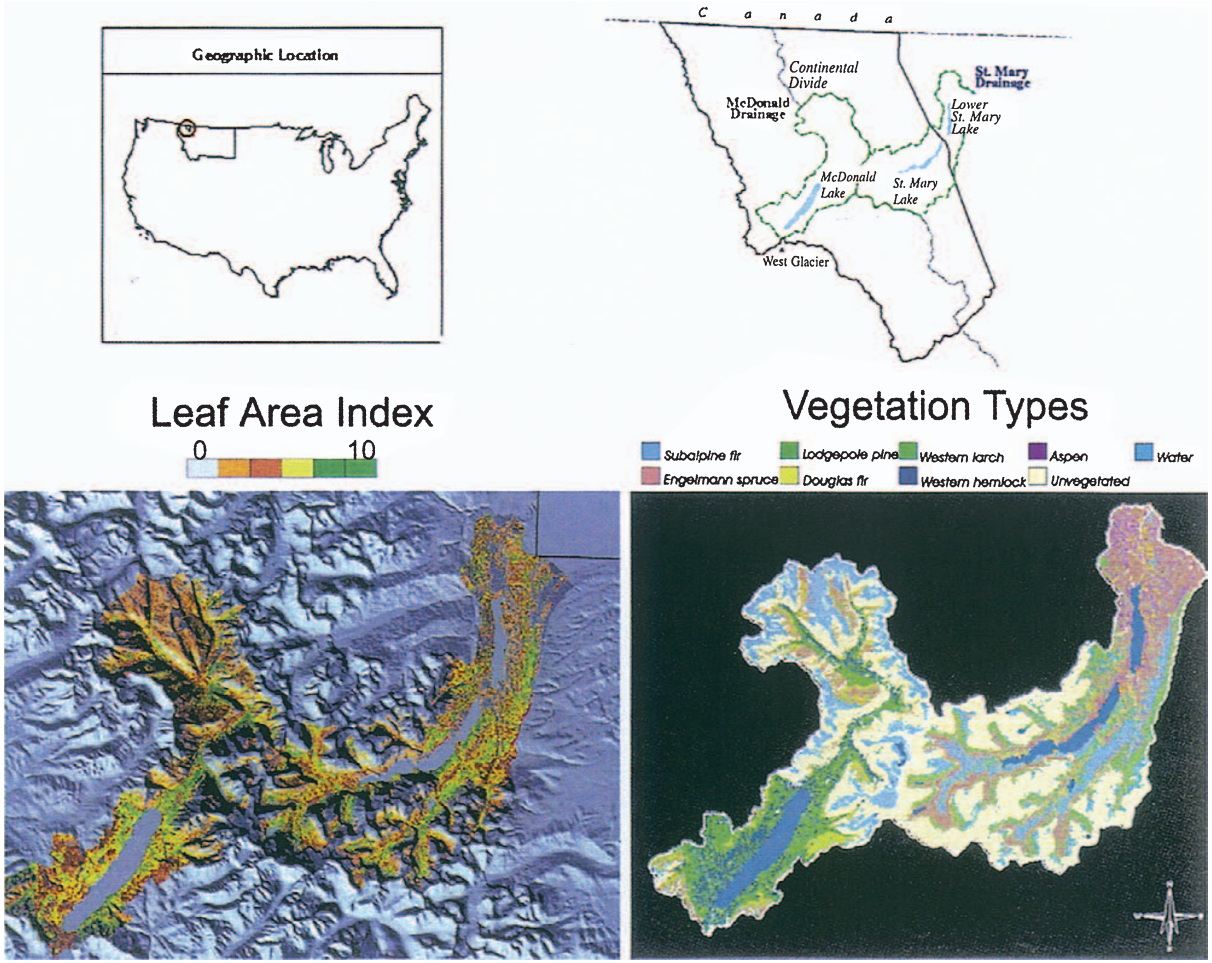

PLATE 7. Definitions of LAI and forest types for two mountainous watersheds straddling the Continental Divide in Glacier National Park, Montana, for the RHESSys simulations in Plates 8 and 9. This 450-km^2 region encompasses elevational ranges from 1000 to 3800 m with orographically induced precipitation ranging from 200 to 2000 mm. Mapping of LAI and classification of the diverse montane forest communities was done with a 15 July 1990 Landsat TM data set. Plate 2 shows the topographic and hydrologic partitioning of the landscape produced as input data layers for a RHESSys simulation. (From Joseph White, University of Montana, and Robert Keane, USDA Intermountain Fire Science Laboratory, Rocky Mountain Research Station, Missoula, MT.)

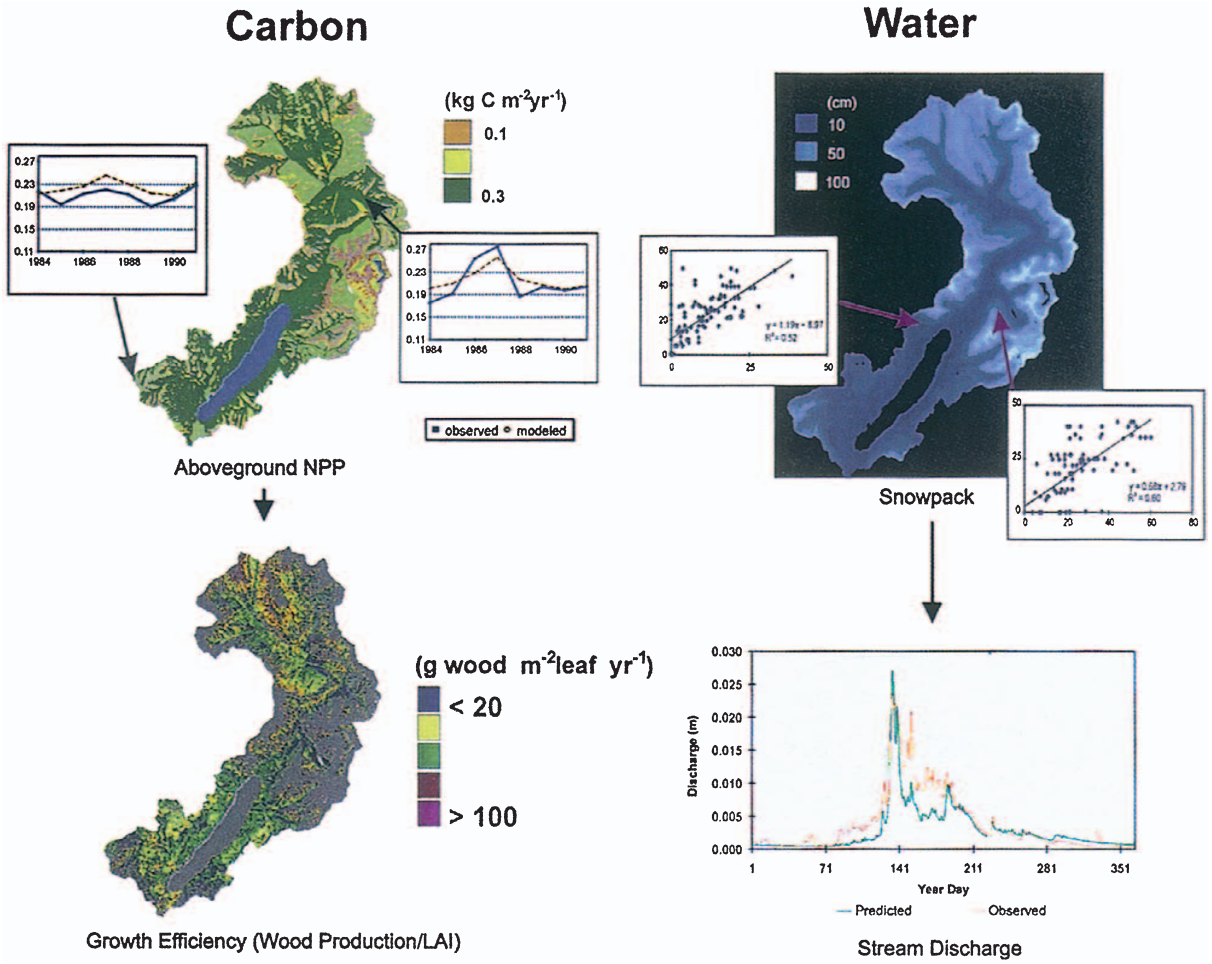

PLATE 8. Seasonal carbon and water budgets simulated by RHESSys for the Glacier National Park study area, with accompanying validation data collected from sites within the watersheds. The 10-year carbon balance simulations were compared to stem growth increment data at two sites in the McDonald Creek watershed (inset graphs). The mid-elevation site showed higher productivity and interannual variability than the southwest facing site. Growth efficiency is simulated to be highest on the south to southeast facing slopes at low elevations where temperatures and incident solar radiation combine to produce the most favorable microclimate in this energy-limited mountain landscape. Stream discharge peaks during the May snowmelt period, and predicted versus observed snowmelt results are inset for two plots in the watershed. (From White *et al.*, 1998)

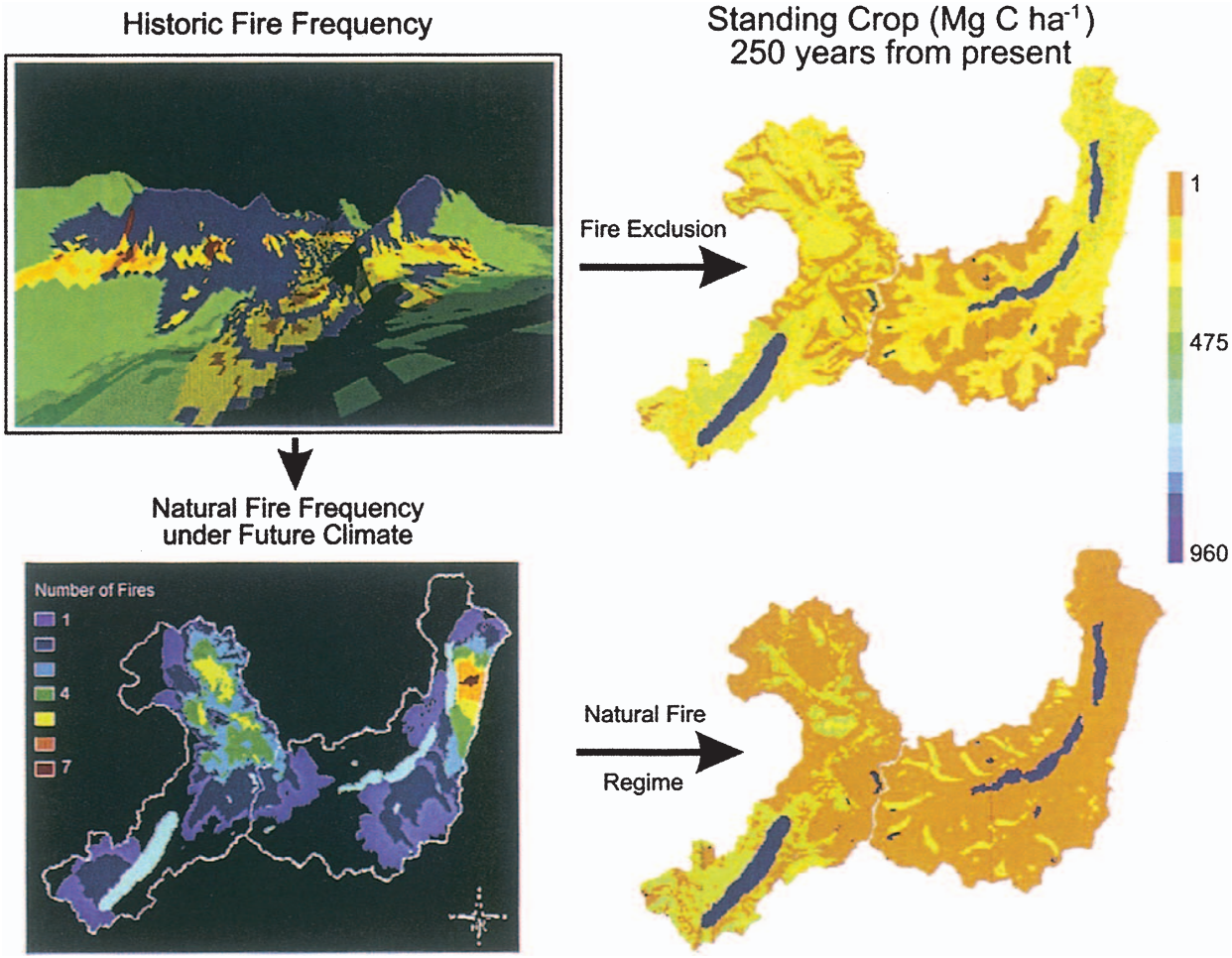

PLATE 9. The stand dynamic model FIRE-BGC (which combines a gap succession model, see Fig. 5.24, and FOREST-BGC) was embedded in RHESSys, and landscape dynamics were studied over a 250-year simulation (Keane *et al.*, 1996a,b). When the model incorporated the historic fire frequency, as high as 7 ignitions as 250 years, much lower standing forest biomass resulted, with higher net primary productivity, compared to a landscape with total fire exclusion. (From Joseph White, University of Montana, and Robert Keane, USDA Intermountain Fire Science Laboratory, Rocky Mountain Research Station, Missoula, MT.)

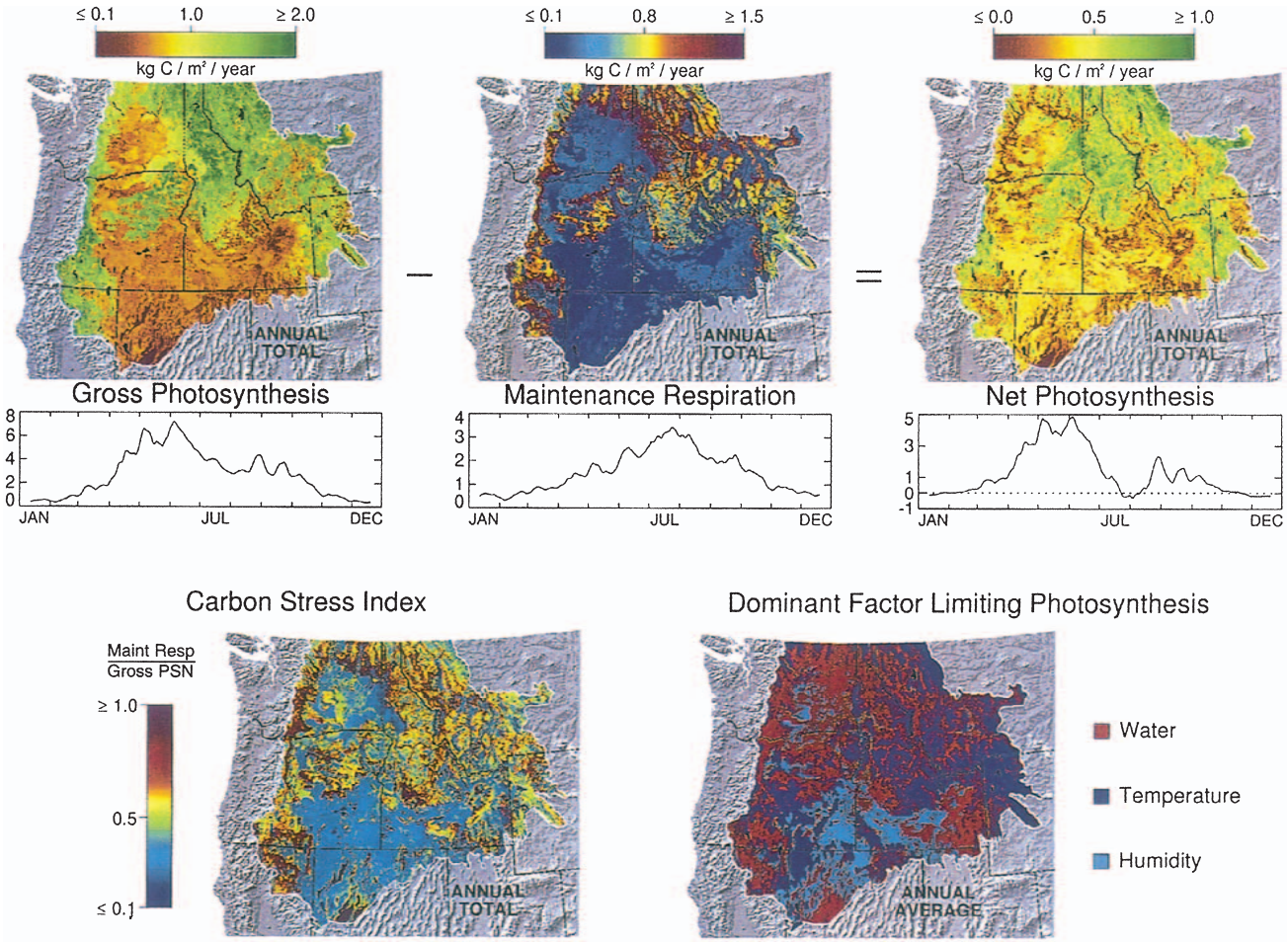

PLATE 10. Comprehensive annual carbon budget for 1989 simulated for the 820,000-km^2 Columbia River basin of the U.S. Pacific Northwest with RHESSys. Seasonal dynamics of each variable averaged for the entire basin are also shown. The extreme climatic diversity of this region is shown in Plate 3. (From Peter Thornton, University of Montana.)

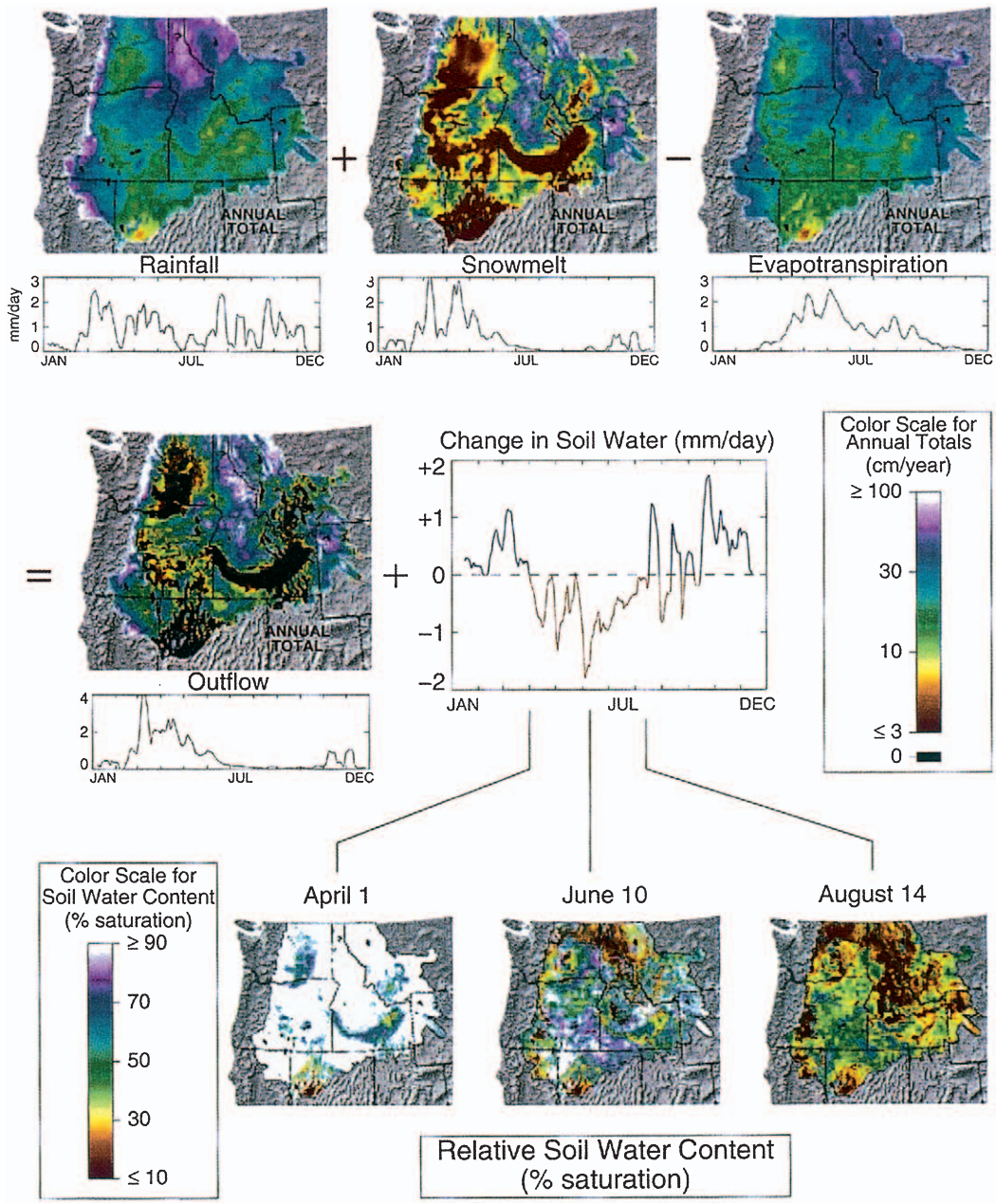

PLATE 11. Comprehensive annual water balance simulated for 1989 over the 820,000-km^2 Columbia River basin with RHESSys. Seasonal dynamics averaged for the basin are also shown. (From Peter Thornton, University of Montana.)